Is Biomass Accumulation in Forests an Option to Prevent Climate Change Induced Increases in Nitrate Concentrations in the North German Lowland?

Stefan Fleck [1,2,*], Bernd Ahrends [2], Johannes Sutmöller [2], Matthias Albert [2], Jan Evers [2] and Henning Meesenburg [2]

[1]   Thuenen Institute for Forest Ecosystems, 16225 Eberswalde, Germany
[2]   Northwest German Forest Research Institute, 37079 Göttingen, Germany; bernd.ahrends@nw-fva.de (B.A.);
     johannes.sutmoeller@nw-fva.de (J.S.); matthias.albert@nw-fva.de (M.A.);
     jan.evers@nw-fva.de (J.E.); henning.meesenburg@nw-fva.de (H.M.)
*   Correspondence: stefan.fleck@thuenen.de; Tel.: +49-3334-3820-376

Abstract: The North German Lowland is a region with locally high nitrate (NO_3^-) concentrations in seepage water, inducing an increased susceptibility to the effects of climate change. The future risk of rising NO_3^- concentrations in seepage water from forests was quantified for four regions in the North German Lowland using climate projections and a modelling system comprising submodels for forest stand development (WaldPlaner), water budgets (WaSiM-ETH), and biogeochemical element cycles (VSD+). The simulations for the period from 1990 to 2070 included three different forest management scenarios (reference, biodiversity, and climate protection) and showed a general decrease in groundwater recharge which could hardly be influenced by any of the management options. The simulated soil organic matter stocks adequately represented their past increase as expected from the National Forest Soil Inventory (NFSI), but also showed a future decline under climate change conditions which leads to higher organic matter decomposition and a long-lasting increase of NO_3^- leaching from forest soils. While the climate protection oriented scenario shows the highest increase in NO_3^- concentrations during the projection period until 2070, the biodiversity scenario kept NO_3^- concentrations in seepage water below the legal thresholds in three of four selected model regions.

Keywords: nitrate; groundwater recharge; climate change; soil organic matter; standing volume; WaSiM-ETH; VSD+; Roth-C; YASSO07

1. Introduction

Next to carbon (C), oxygen, and hydrogen, nitrogen (N) is one of the main building elements of plant biomass, being of central importance for plant metabolism and growth. Since nitrogen is mainly taken up by the roots of plants in the form of soluble nitrate (NO_3^-) or ammonium (NH_4^+), the availability of these ions in the soil solution is a precondition for plant growth and has been a growth limiting site condition in many ecosystems including forests [1,2]. During the last sixty years, atmospheric emissions of N species (NO_x, NH_3) from traffic, industrial processes, and agriculture in Central Europe have been drastically elevated. Subsequent deposition to terrestrial ecosystems increased N availability to a level exceeding the demand of forest stands' growth increment [3]. It has been shown that this long-term increase in N deposition significantly increased forest productivity [4], thereby making forest biomass a valuable sink for excess N. Unfortunately, excess N is usually not completely retained within the forest ecosystems: After a period of N accumulation in the ecosystem, forests may become N saturated and NO_3^- is increasingly leached with seepage water [5,6], causing

increased NO_3^- concentrations in groundwater and surface waters [7,8] and also leading to a loss of base cations relevant for tree nutrition [9]. The oxidation of deposited NH_4^+ in forest ecosystems by plant uptake or nitrification causes the generation of acidity which may subsequently be transferred to surface waters [10,11]. Although N deposition to forests was slightly reduced during the last two decades [12], a high proportion of forest ecosystems in Central Europe shows symptoms of N saturation [3], leading to nutrient imbalances as well as a marked loss of their N retention capacity [13].

Forests play a major role in water quality in the cultural landscapes of Europe [14], because unlike for agricultural land-use, fertilization, the application of pesticides and tillage are nearly absent in forests. Consequently, the NO_3^- concentration in the surface groundwater is usually substantially lower under forest as compared to arable land [15]. The implementation of the EU Water Framework Directive (WFD, [16]) requires integrative concepts to ensure a good quality of seepage and groundwater. The limitation of NO_3^- leaching is one of the key objectives of the WFD where a legal threshold of 50 mg L^{-1} was set as the maximum acceptable NO_3^- concentration in surface and groundwater [16,17]. As atmospheric deposition is the major input flux of N in forest ecosystems, it often determines, to a large degree, N output [18]. However, tree biomass, forest floor, and mineral soil are important ecosystem compartments that may retain huge amounts of N and significantly delay the effects of atmospheric N input on N leaching in forests [13,19–21]. Some studies show that the C/N ratio of the forest floor or the upper mineral soil can be a valuable indicator of the risk of NO_3^- leaching from forest soils [18,22,23].

As temperature and water availability are important drivers for processes involved in the N cycle, climate change is expected to have a considerable potential for the alteration of ecosystem N fluxes and in particular for the N retention in the soil [24]. Relative to 1850–1900, global circulation models (GCMs) project increases of the global mean annual surface temperature for the end of the 21st century between 1.0 and 5.5 K [25,26]. Several modelling approaches have been employed to assess deposition scenarios and climate change impacts on forest soils including NO_3^- leaching [27,28]. However, there is often a gap between models intended for systems understanding and models for decision support, hampering their application for practical purposes [29].

The present study pursues (i) an evaluation of the effects of the intensity of forest management on NO_3^- concentrations and leaching for selected model regions in the North German Lowland and (ii) an assessment of future risks for NO_3^- leaching under changing climatic conditions. In order to achieve these aims, we implemented a scale-independent modelling framework. The study has been conducted within the framework of the project Sustainable Land-Use Management in the North German Lowlands (NaLaMa-nT, [30,31]).

2. Materials and Methods

The study area comprises the North German Lowland, a mainly plain, sometimes undulated landscape with only low elevations. The landscape is formed by Pleistocene and Holocene sediments. Agricultural land-use prevails, but a considerable area, which is increasing from west to east, is forested. Climate is temperate with maritime influence in the northwestern parts and subcontinental influence in the southeastern parts.

2.1. Model Regions

Four model regions were selected for the study, representing the existing spatial gradients in continentality, N deposition, proportion of organic soils, and soil fertility in the North German Lowland. For these regions, it was possible to obtain the required retrospective and prospective data on forest stands, site conditions, and climatic drivers in a high spatial and temporal resolution in order to implement the modelling system for the simulation of forest stand development and N cycling. Measured and simulated stream chemistry data for selected catchments in the model regions are available as additional information [32].

The model region Diepholz (acronym DH) with a forested area of 15,042 ha, equaling 6.7% of its total area, is characterized by a maritime climate with 743 mm annual precipitation and a mean temperature of 9.7 °C, high N deposition from intensive agriculture (40 kg ha^{-1} a^{-1}) with an NO$_x$/NH$_y$ ratio of 0.3), and a high proportion (in area) of organic forest soils, soils with predominantly high field capacity, and a large part of the forested area with connection to groundwater (42% $\leq$ 2.5 m depth to groundwater level). Tree species composition in DH is very diverse with 65% deciduous and 35% coniferous species. The majority of forest stands are relatively young (approx. 60% between 20 and 60 years).

The county Uelzen (acronym UE) comprises a forested area of 45,712 ha (34.7% of its total area) and is located within a still maritime climate with subcontinental impact and a mean annual temperature of 9.3 °C.; its annual precipitation being 721 mm, only slightly lower than that of the more maritime region Diepholz. Only 9% of its forest soils have connection to groundwater, the soils being mainly sandy with medium to low soil water availability. Nitrogen deposition is 26 kg ha^{-1} a^{-1} (NO$_x$/NH$_y$ = 0.7), slightly above the average for the North German Lowland. Tree species distribution is strongly influenced by Scots pine (61%) and deciduous species account for only 20%. The age class distribution is predominated by stands aged 40 to 80 years (approx. 60%).

The model region Fläming (acronym FL; 51,368 ha forests, 41.5% of total area), in contrast, is exposed to a subcontinental climate and local emissions of N compounds (NO$_x$/NH$_y$ = 0.6, on average 25 kg ha^{-1} a^{-1}). This model region receives (except on the top of hills) a very low amount of precipitation (long-term average 1991–2010: 572 mm). Mean annual temperature is 9.8 °C. Only 11% of the predominating sandy soils are connected to groundwater. The predominance of Scots pine increases from west to east. In FL, it already accounts for 74% of the forest area. Approx. 23% of the area is deciduous trees, especially European beech and sessile and pedunculate oak. The age class distribution in FL is almost balanced.

The model region Oder-Spree (acronym OS, 76,714 ha forests, 48.7% of total area) is also exposed to a subcontinental climate with very low precipitation (long-term average: 572 mm). Mean annual temperature is 9.6 °C. While the predominantly sandy soils have low field capacity, groundwater is accessible in 22% of the forested area for tree roots (<2.5 m depth). Nitrogen deposition is comparatively low in this model region with 22 kg ha^{-1} a^{-1} and a NO$_x$/NH$_y$ ratio of 0.8. In OS, Scots pine covers 81% of the area and only 17% is deciduous species. Approx. 70% of the stands are between 40 and 100 years old.

2.2. Climatic Data and Climate Projections

Retrospective and prospective climatic data were obtained from the output of an ensemble of 21 global circulation models (GCM) based on the RCP 8.5 emission scenario [33,34]. With regard to the most recent years since 2010, out of all RCP scenarios, the RCP 8.5 emission scenario fits best to current emissions. The regional climate projections for the four model regions differed between the GCMs mostly in the projected mean annual temperature increase for the period 2050–2070, which varied between 1.1 K and 2.7 K. The projected change in annual precipitation varied between −220 mm and +218 mm for a period of 100 years (on average +14.6 mm) over all projections. We considered the median run with respect to climatic water balance—due to the high relevance of water seepage for the investigated processes—for further analyses. The selected climate projection is based on the GCM ECHAM6 [35].

The output of ECHAM6 was downscaled to the 2236 climate stations of the German Weather Service (DWD) using the regional climate model STARS [36] to obtain daily values of precipitation, sunshine duration, mean temperature, relative humidity and wind speed for the period 1991 to 2070 for Germany, which were further downscaled to a 100 m grid using a combination of inverse distance-weighting and an elevation-dependent regression implemented in the hydrological model WaSiM-ETH [37]. The STARS statistical model creates climate projections based on a temperature-conditioned resampling in order to estimate climatic elements for a given temperature

increase [38]. The temperature dynamic is defined as a periodic trend obtained by the GCM. The resampling is done in two steps. Firstly, by the means of newly arranged annual climate values and secondly by a rearrangement of 12-day weather sequences.

The climatic time series for the retrospective period 1991 to 2010 generated with STARS was compared to observed data from the DWD and produced a climate scenario with less than 0.1 °C deviation from the annual mean temperature in each model region and a slightly lower precipitation (-1% to -5% relative to measured values for that period). The use of simulated climate data also for the past period enabled a better consistency of the analysis over the whole simulation period.

2.3. Forest Management Scenarios

Three different options of future forest management were considered as management scenarios, hereafter referred to as 'reference', 'biodiversity', and 'climate protection' scenarios. The reference scenario reproduces close-to-nature silvicultural practices which are widely applied in northern Germany today (e.g., LÖWE, [39]). Close-to-nature silviculture favours the cultivation of broadleaf trees and mixed species stands, always considering the selection of site-adapted species. The biodiversity scenario favours tree species of the potential natural vegetation (PNV) and reduces the maximum allowed harvest volume from 70 to 50 m^3 ha^{-1} per cut. PNV trees are allowed to grow 5 to 10 cm larger in target diameter and introduced tree species are felled when they are 5 to 10 cm smaller in target diameter than in the reference scenario. Thus, in the biodiversity scenario, thinning volume is less and final harvests are delayed compared to the reference scenario. Dead wood is accumulated up to 40 m^3 ha^{-1} instead of only 20 m^3 ha^{-1} in the other two scenarios. Furthermore, under the biodiversity scenario, 5% of the forest area remains unmanaged while under the reference and climate protection scenario the unmanaged area ranges from 1% to 2% depending on the model region. The third scenario is termed climate protection, since it aims to maximize C storage in standing biomass and wood products. It favours fast-growing site-adapted coniferous trees with a 5 cm smaller target diameter compared to the reference scenario. Consequently, under the climate protection scenario, more volume is cut and final harvest is at an earlier stage compared to the reference scenario.

2.4. The Modelling System

The modelling system is based on well documented, publicly available models for forest growth, water budgets, and biogeochemical matter cycling. The individual models were externally coupled in such a way that the output of the models, necessary as the input for the other models, is exchanged at the beginning of each simulation cycle. Details on the coupling procedure between the hydrological and forest growth model are given in [40]. The individual models are established and validated models and were adapted to the purpose of this study. Therefore, we present only a short overview of each model.

2.4.1. Forest Growth Model

To model the growth of the forest stands, we employ the statistical individual tree growth model TreeGrOSS parameterized using data from Northwestern Germany [41]. For this study, TreeGrOSS was extended by implementing a climate-sensitive longitudinal diameter–height model [42]. The model, originating from a re-parameterized version of the Korf function by Lappi [43], predicts single-tree height to diameter relations as a function of soil and climate parameters (cf. [30,42]). The longitudinal diameter–height model is spatially explicit, thus it takes, among others, the strongly spatially correlated nitrogen deposition into account. TreeGrOSS and its climate-sensitive extension are the core for the forest simulation system "WaldPlaner 2.1" [41]. The WaldPlaner system projects forest development by applying silvicultural management regimes and accounting for changing climatic conditions. The system requires data on forest stands, soil properties and climate conditions as the input and silvicultural management regimes are specified using a list of control variables [30]. The control

variables used in the forest growth simulator WaldPlaner to define the management scenarios are listed in Table 1.

Table 1. Characteristics of selected control variables defining the three silvicultural management scenarios' reference, biodiversity and climate protection in the forest growth simulator WaldPlaner.

Control Variable	Reference	Biodiversity	Climate Protection
unmanaged area	status quo	5% of forest area	status quo
area under flora-fauna-habitat (FFH) directive	45% of the FFH-area as natural habitat type	100% of the FFH-area as natural habitat type	45% of the FFH-area as natural habitat type
deadwood (m³/ha)	20	40	20
selection of future stand type	dominating deciduous species	tree species of potential natural vegetation (PNV)	dominating conifer species
thinning intensity	variable over time: high, moderate, low	moderate	variable over time: high, moderate, low
thinning type	thinning from above	thinning from above	thinning from above
start of thinning (defined by stand height)	12–16 m	12–16 m	11–15 m
limit of thinned volume per cut (m³/ha)	max 70 (Douglas-fir max 100)	max 50 (Douglas-fir max 100)	max 70 (Douglas-fir max 100)
target diameter (cm)	oak 70, beech 60, spruce 45, pine 45, Douglas-fir 70	all species +5 cm, in FFH-areas +10 cm, except spruce −5 cm, Douglas-fir −10 cm	all species −5 cm
limit of harvested volume per cut (m³/ha)	max 100 (Douglas-fir max 120)	max 70 (max 100 for all species not included in PNV)	max 100 (Douglas-fir max 120)

The initialization of forest stands for the forest growth model was based on forest authority data from the currently existing forests at roughly 1000 randomly chosen locations along a regular grid over each model region (altogether 3883 sampling points). Due to lacking of some data and the low proportion of forested area in the model region Diepholz, the number of sampling points was lowest in this region (874), while it was between 999 and 1008 for the other regions. The initialization data from these points comprise stand age, tree species composition, and for each species and stand layer its coverage, mean diameter at breast height (DBH), mean height, age, volume per ha, and relative stand density [31].

At the beginning of a simulation cycle, the WaldPlaner system generated model stands with individual trees based on stand parameters as listed above for each sampling point in the model regions. For each single tree, tree characteristics such as age and DBH were calculated and entered into the database. The stand development and consequently the tree dimensions are updated in 5-year prediction intervals. Besides the forward projection of stand development, it was also necessary to reconstruct forest development by backward simulations with the WaldPlaner system for the past period 1991 to 2010.

The same approach for the initialization of stands was chosen for plots of the National Forest Soil Inventory (NFSI) in the North German Lowland based on inventory data from 2012.

A comprehensive system of rules, implemented in the database, was followed to determine all stand-specific parameters from single tree data and process them for the submodels. The degree of canopy cover was calculated directly for each stand in WaldPlaner, with values ranging between 0 and 100% (complete canopy cover). If less than 85% of the stand area was under canopy cover, a secondary vegetation layer (ground vegetation) was considered. Due to an extended vegetation period as a result of changing climate conditions, we expected a changing phenology of the trees. Therefore, we calculated the vegetation period for each year separately. The start of the vegetation period was determined using a degree-day model of Menzel [44]. The termination of the vegetation period was estimated according to von Wilpert, Walther and Linderholm, and Frich et al. [45–47]. Thus, the termination of the vegetation period is based on either the short-day criterion or the temperature criterion, whichever is met first. Von Wilpert [45] selects 5 October as the short-day criterion, as day length after 5 October is not sufficient to warrant xylem growth. The temperature criterion is met

according to Walther and Linderholm as well as Frich et al. [46,47], when the moving temperature average within a 7 day span falls below 5 °C. The maximum leaf area index (LAI) was derived for each tree species based on allometric relationships [48]. As the growth model indirectly accounts for nitrogen deposition, LAI is affected as well. The forest characteristics were also coupled with the GrowUp model [49]. It is a pre-processor for VSD+ to compute nutrient uptake and litterfall from tree growth data. For nutrient content in tree compartments, data from [50] were used. The foliar N content is modelled depending on nitrogen deposition (cf. [49]).

2.4.2. Water Budget Model

The WaSiM-ETH model [37] was used to calculate the water budget at each sampling point of the model regions, driven by the projected climate data. The model uses grid-based information for meteorological drivers, site and stand characteristics. The model has been run on a daily time step. It was parameterized based on the forest inventory data of the year 2010 (leaf area index LAI, stand height, canopy cover) and forward and backward calculated forest stand dynamics from the WaldPlaner simulations. The LAI (comprising all plant surfaces, i.e., including stems and ground vegetation) of coniferous forest stands during the dormant season has been set to 80% of the maximum LAI and for deciduous forest stands to 50%. Soil water fluxes are simulated using a one-dimensional form of the Richards equation. Parameterization of soil water retention functions has been carried out according to van Genuchten [51]. The van Genuchten parameters have been obtained using soil information from a digital soil map (Forest-BÜK 1:1 Mio, [52]) and pedotransfer functions from [53]. The calculated seepage rate equals the amount of water that leaves the lowest simulated soil layer below the rooting zone and was assumed to represent the groundwater recharge.

An additional and spatially more extended simulation assuming static forest stand conditions was performed for the plots of the NFSI in Brandenburg, Saxony-Anhalt, Lower Saxony, and Schleswig-Holstein, where observed soil and stand information spread over large parts of the North German Lowland was available. This simulation serves as a baseline that allows to disentangle climatic effects from effects of stand development.

2.4.3. Element Budget Simulations

The VSD model (Very Simple Dynamic) has proven to be suitable to describe the dynamics of the acid-base status [54,55], and C and N dynamics of forest soils, e.g., for ICP Forests Level II plots in Germany [56–61]. The VSD model was chosen in this study due to its relatively low data requirements and the limited data availability in the model regions.

The dynamic development of C and N stocks within the organic layer and the upper 90 cm of the mineral soil was calculated with VSD+ version 5.2; Coordination Centre for Effects (CCE), Bilthoven, The Netherlands, [62,63], including the C model Roth-C [64] as an integrated submodel. For comparison, C dynamics in soil organic matter were additionally calculated with the model YASSO07 [65]. Aboveground and belowground litter input for both models were derived based on the model GrowUp (version 1.3.2; CCE, Bilthoven, The Netherlands, [49,66]) in which biomass expansion factors and turnover rates used in the EFISCEN model [67] were implemented. Climate and soil water conditions as well as stand characteristics are based on the climate projections and water budget and forest growth simulations described above. The N uptake efficiency (Nupeff) in the VSD+ model is an essential parameter representing the fraction (-) of N deposition that is available for uptake. The default value for Nupeff is 0.92 [63] which implies that 8% of deposited N will be leached e.g., during the dormant season [61]. We chose somewhat higher values between 0.96 and 0.99, assuming that the N leaching is less pronounced in regions with relatively low rainfall (cf. Chapter 2.1) [68].

The full list of parameters used for the VSD+ model is given in Appendix A. The N fluxes calculated with VSD+ were balanced to yield the N budget of the forest soil:

N budget = N deposition + N litter input − N uptake − N leaching − N losses by denitrification

Carbon and N stocks were initialized using data from the first NFSI with the reference year 1991 [69,70]. The initial distribution of soil organic matter content among the five C pools is done by assuming that the inert organic matter can be estimated from the total organic matter contents according to [71].

Initial soil C stocks for YASSO07 were also derived from the first NFSI. However, its distribution among the five pools cannot easily be estimated and an unbalanced pool initialization may result in unrealistic model output [72]. Therefore, the model pools were initialized using a spin-up procedure [73] running the model for 1000 years backwards with dynamic litter inputs from yield tables and constant climatic conditions (mean average temperature and drought index for the regions).

The performance of both C models was evaluated based on the observed soil C dynamics between the first and the second NFSI that was regionalized with a generalized additive model (GAM, see below and Figure 5).

2.5. Spatially Explicit Input Data

The model system described above needs a set of input data for the sampling points in the model regions that includes soil properties, N deposition, and climate characteristics. The simulations are run for each point. The physical soil characteristics are assumed to be static over the considered time, whereas the chemical soil parameters are calculated dynamically with VSD+. N deposition was included as a time series derived from air pollution abatement scenarios (see Section 2.5.2).

2.5.1. Soil Data

Physical soil properties (soil texture, bulk density, stone content, available soil water capacity, etc.) were taken from a digital soil map of scale 1:1 Mio (Forest-BÜK, [52]). More details can be found in Albert et al. [31]. Potential cation exchange capacity was calculated with pedotransfer functions of Müller and Waldeck [74].

The soil chemical input parameters (C and N stocks, base saturation) were regionalized for each sampling point with generalized additive models (GAMs) built on the evaluation of NFSI data. Statistical correspondence between 185 variables of the NFSI (Appendix B) was condensed in three GAMs in order to enable the regionalization of C and N stocks, as well as base saturation, for the sampling points for the reference years 1991 (first NFSI) and 2006 (second NFSI) based on available parameters from the digital soil map (potential cation exchange capacity, soil type, bedrock, forest type, soil region, proportion of coarse fragments, mean annual temperature, N and S deposition, degree of podsolization). Parameter selection followed a maximum likelihood based approach (R-package mgcv [75,76]). Here, continuous variables were represented as tensor product approximations with restricted curve flexibility. The exhaustive dataset of the second NFSI was used for parameter selection, whereupon the first NFSI was used as an independent dataset to test the validity of the model structure for another point in time.

The regional transfer model for organic C stocks (forest floor plus mineral soil up to 90 cm depth) has the form

$$\text{gam}(C_{org}) \sim \text{te}(CEC_{pot}) + \text{te}(N_{dep}) + \text{te}(GC) + \text{te}(T) + BR + Stype + Sregion + stand,$$

with C_{org} depending on four continuous variables: potential cation exchange capacity (CEC_{pot}), N deposition (N_{dep}), gravel content (GC), and annual mean Temperature (T), as well as on four classified variables: bedrock type (BR), soil type and soil region according to the German soil classification system (Stype and Sregion, [77]), and stand type classification (broadleaf, coniferous or mixed stand). Bedrock types were distinguished between basic bedrock, acidic/intermediate bedrock, silica based bedrock, sandstone, organic formations, and unconsolidated rock. Soil types were classified into carbonatic immature soils, lessive soils, podsols, anthropomorphic soils, and other soils.

The quantification of C/N ratios for VSD+ required an additional regional transfer model for N stocks within the same soil depth. Parameter selection resulted in the following model:

$$gam(N) \sim te(CEC_{pot}) + te(C_{org}) + Pod + BR + te(hum) + broadleaf$$

Here, the continuous variable (hum) stands for thickness of the forest floor, and additional classified variables are degree of podsolization (Pod) and purely broadleaved stand vs. other stands (broadleaf). Next to CEC_{pot} and C_{org}, each of the four degrees of podsolization was a significant variable with $p \leq 0.001$.

Base saturation from NFSI plots was integrated over 90 cm of the mineral soil and forest floor considering soil bulk density, amount of fine earth and thickness of the soil layer as weighting factors (cf. [78]). This integrated base saturation (BS) was regionalized with the model

$$gam(BS) \sim Carbonate + dBR + te(CEC_{pot}) + Pod + te(S_{dep}) + Sregionclass,$$

where Carbonate means the presence of carbonates within the upper 90 cm of the mineral soil or the forest floor. dBR stands for the dominant bedrock type: While the existence of basic, carbonatic, or acidic bedrock and organic materials among the parent material was automatically considered as dominant, intermediate magmatic bedrock, non-carbonatic unconsolidated rock, intermediate/basic metamorphous bedrock, and silica-based bedrock was only considered dominant if the former types were absent. S_{dep} is the average S deposition over 4 years (1990–1993 for the first NFSI and 2004–2007 for the second NFSI) and Sregionclass is soil region according to AG Boden [66]; however, combining all mountainous soil regions (classes 8–11) into one class and all other morainic or loess-dominated soil regions (classes 3–7) into another class, next to the stream valleys (class 2) as a third class. When this GAM was applied to data from the second NFSI, all single degrees of podsolization, carbonate, and CEC_{pot} are significant variables with $p \leq 0.001$ and S_{dep} is significant with $p \leq 0.01$. Sregionclass was significant with $p \leq 0.05$, but strongly lowered spatial autocorrelation (Moran's I = 0.26). Overdispersion of the base saturation data required the use of a quasibinomial error distribution function.

2.5.2. Deposition

Following [27], the long-term trends for the deposition of N, sulphur (S) and base cations were calculated with the model MAKEDEP [79]. The model was run with grid-based estimates of Builtjes et al. [80] for a period from 2004 to 2007. To reconstruct the deposition before 2004, we used the regional trend from the EMEP database [81] and standard time series from Alveteg et al. [79]. Annual deposition from 2007 to 2020 was estimated according to the National Emission Ceilings for Europe [82] assuming constant regional distribution of deposition and taking changes in tree species composition in the model regions into account. The N emissions were assumed constant from 2020 onwards.

2.6. Statistical Analysis

All statistical analyses were performed using the statistical software R [83] in combination with the packages mgcv [75,76] and ape [84] to investigate spatial autocorrelations (Moran's I).

3. Results

Results are presented as means aggregated over 20-year periods from 1991 to 2070 in order to enhance the visibility of long-term trends and to eliminate the inter-annual variations of climate projections.

3.1. Standing Volume and Species Composition

In OS, the initial mean standing volume of 275 m^3 ha^{-1} is highest, followed by 263 m^3 ha^{-1} in FL and 261 m^3 ha^{-1} in UE. Due to the predominance of young stands, the initial mean standing volume in DH is rather low with only 175 m^3 ha^{-1} (Figure 1). For all four model regions, the projected stand development until 2070 shows the highest standing volume for the biodiversity scenario, and the

lowest values for the climate protection scenario and the reference scenario in an intermediate position. In DH, starting from a low level, standing volume accumulates over time; a slight decrease is only projected between 2051 and 2070 for the climate protection scenario. In UE, an increase in standing volume is projected for all management scenarios for the 2010 to 2030 period. A volume reduction is projected for the climate protection scenario after 2030 and for the reference scenario after 2050. In FL and OS, the development of standing volume is quite similar: For the biodiversity scenario, a steep increase until 2050 and a marked decrease afterwards was simulated. Due to the age stratification of forest stands in FL, stand development differs clearly between the three management scenarios: While standing volume decreases continuously in the reference scenario, the biodiversity scenario leads to increasing forest biomass until 2050 and biomass reductions due to aging stands thereafter. The climate protection scenario projects a strong decrease in standing volume at the beginning due to reduced harvesting dimensions and higher allowable cuts, followed by an increase in standing volume after 2050 when newly established stands with mainly fast-growing conifer species contribute considerably to the regional standing volume. In the reference scenario, standing volume is decreasing until 2070, but reduction is not so strong and is distributed over a longer period compared to the climate protection scenario.
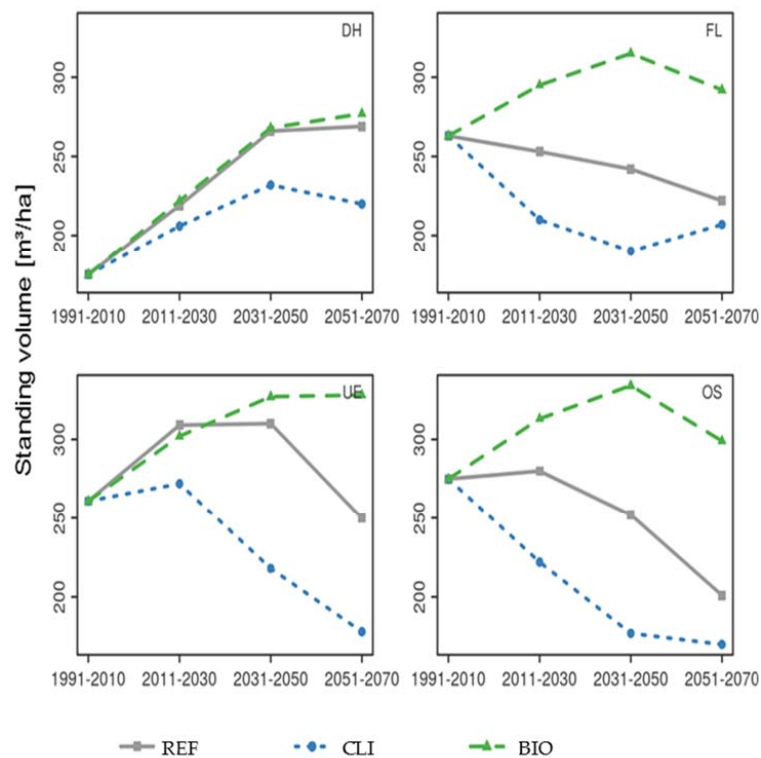

Figure 1. Simulated development of standing volume in the four model regions: Diepholz (DH), Fläming (FL), Uelzen (UE), and Oder-Spree (OS) under the three silvicultural management scenarios: reference (REF), climate protection (CLI), and biodiversity (BIO) until 2070.

An assessment of the uncertainty in the volume estimates (Figure 1) due to underlying climate projections is given in [31].

Table 2 displays the influence of the three management scenarios on tree species distribution until 2070. Generally, the proportion of Scots pine decreases in all regions and all management scenarios with the exception of DH, where an increase is projected even for the biodiversity scenario. The climate protection and reference scenarios cause an increase of Douglas-fir at all model regions. Beech and, to a lesser extent, oak also show increasing proportions under all management regimes in all regions, except oak in UE.

Table 2. Proportion of species crown cover based on the forested area of the respective region for European beech, sessile and pedunculate oak, all other deciduous species, Norway spruce, Scots pine, Douglas-fir and all other coniferous species in 2010 and change in percentage points until 2070.

		Beech	Oak	Other Deciduous	Spruce	Pine	Douglas-Fir	Other Conifers
DH	2010	8.9%	11.2%	45.2%	6.0%	19.3%	4.1%	5.4%
	REF 2070	+5.1	+2.1	−4.7	−0.8	−0.9	+1.1	−2.0
	CLI 2070	+7.8	+3.0	−25.0	+2.1	+7.4	+5.9	−1.4
	BIO 2070	+0.2	+4.6	−2.5	−2.2	+2.8	−1.5	−1.5
UE	2010	4.8%	6.1%	8.7%	13.3%	61.3%	3.9%	1.9%
	REF 2070	+7.0	+1.6	+2.3	−6.7	−17.7	+13.3	−0.1
	CLI 2070	+14.7	−0.9	−1.5	−8.9	−34.1	+26.8	+4.0
	BIO 2070	+8.0	+0.2	+0.6	−5.6	−3.2	+0.4	−0.4
FL	2010	12.8%	5.9%	4.3%	1.8%	73.5%	0.4%	1.2%
	REF 2070	+8.3	+2.5	−0.4	−0.8	−11.2	+1.9	−0.2
	CLI 2070	+8.4	+1.9	−1.2	−1.1	−30.2	+18.5	+3.8
	BIO 2070	+5.9	+0.7	+1.1	+1.6	−9.2	±0	±0
OS	2010	2.0%	5.7%	8.8%	1.1%	80.9%	0.5%	1.0%
	REF 2070	+7.1	+2.9	−1.8	−0.1	−8.3	+0.3	−0.1
	CLI 2070	+7.1	+3.4	−3.8	−0.2	−23.1	+12.9	+3.6
	BIO 2070	+0.7	+0.4	+0.7	+0.4	−2.1	−0.1	+0.1

DH (Diepholz), UE (Uelzen), FL (Fläming), and OS (Oder-Spree) represent the respective model region; REF (reference), CLI (climate protection), and BIO (biodiversity) are the management scenarios applied.

3.2. Groundwater Recharge

3.2.1. NFSI Plots (Static Forest Stands)

Under current (1991–2010) climate conditions, groundwater recharge in the lowlands of Schleswig-Holstein and Lower Saxony is mostly high (>100 mm) or very high (>200 mm), while it is only low (<50 mm) or very low (<25 mm) in the lowlands of Brandenburg and Saxony-Anhalt (Figure 2). This is a consequence of the marked precipitation gradient from the Northwestern to the Southeastern part of the North German Lowland. Groundwater recharge under future (2051–2070) conditions of the RCP 8.5 scenario (but assuming constant forest stand characteristics) will generally be considerably lower, with many NFSI plots where groundwater recharge is missing except for wet years. Few NFSI plots are directly located within the four model regions. Those in DH exhibit groundwater recharge of currently 225 mm and 145 mm in 2051–2070. In UE, groundwater recharge would decrease from currently 255 mm to 180 mm assuming constant stand characteristics. In FL and OS, where seepage was only medium under current conditions, it decreases from 90 mm to 55 mm and from 100 mm to 50 mm, respectively.
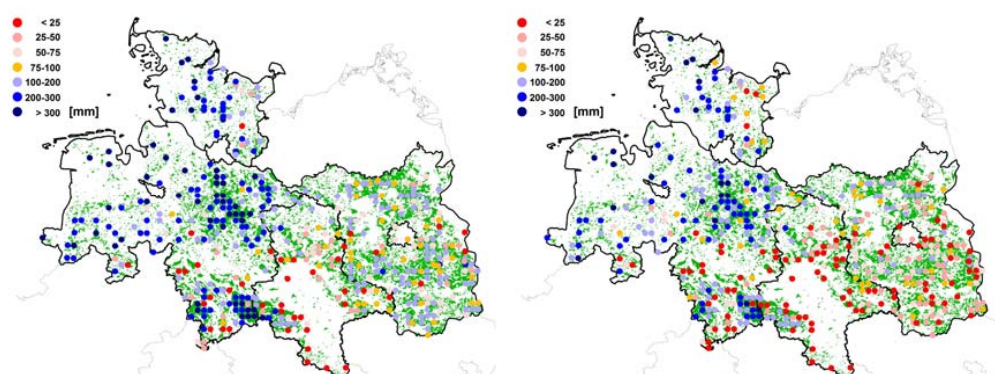

Figure 2. Average annual groundwater recharge on plots of the second National Forest Soil Inventory (NFSI) in Brandenburg, Niedersachsen, Sachsen-Anhalt, and Schleswig-Holstein under current 1981–2010 (**left**) and projected 2041–2070 (**right**) climate conditions.

3.2.2. Sampling Points in Model Regions (Dynamic Stands, cf. Figure 3)

1. Diepholz (DH)

Based on the RCP 8.5 scenario, the annual precipitation (close to 800 mm) at sampling points in DH remains almost unchanged until 2070. Average groundwater recharge in this region decreases from 138 mm (1991–2010) to 59 mm in 2051–2070 in the reference scenario. For the biodiversity scenario and the climate protection scenario, the values for groundwater recharge in the 2051–2070 period are 56 mm and 64 mm, respectively.

2. Uelzen (UE)

Precipitation remains almost unchanged in UE similar to DH, but groundwater recharge is generally higher (between 210 mm and 260 mm), since the sandy soils have a low water storage capacity. Groundwater recharge remains almost constant over the simulation period for all management scenarios with a slight decrease towards the end of the simulation period due to increasing evaporative demand. A small difference between the biodiversity scenario (214 mm) and climate protection scenario (222 mm) was simulated for the period 2051–2070.

3. Fläming (FL)

Annual precipitation in this region (600 mm) will slightly increase in 2011–2030 and 2031–2050 according to the RCP 8.5 scenario followed by a decrease to 580 mm in the last 20 years of the simulation period. Similarly, groundwater recharge with 65 mm is low from the beginning and remains constant until 2050, but decreases—parallel to decreasing precipitation—to 22 mm in 2051–2070. The marked differences in standing volume between the three scenarios only have marginal influence on the decreasing trend in groundwater recharge. The aging stands in the biodiversity scenario reduce the evaporative demand due to lower LAI and thereby allow higher annual groundwater recharge of 32 mm in 2051–2070, while the strong growth of young Douglas-fir stands (established in the simulation period) in the climate protection scenario reduce groundwater recharge in 2051–2070 to only 13 mm. All scenarios have in common the absence of groundwater recharge at many sampling points in dry years.

4. Oder-Spree (OS)

Low annual precipitation rates of 630 mm lead to groundwater recharge of, on average, 80 mm throughout the years from 1991 to 2050. During the last 20 years of the simulation period, when the projected precipitation rate decreases by 50 mm, the groundwater recharge decreases by 40 mm. The difference between the reductions of precipitation and groundwater recharge (10 mm) is compensated by a reduced evapotranspiration rate. The effect of older forest stands in the biodiversity scenario has only little influence on groundwater recharge (45 mm in 2051–2070), and the high transpiration of growing Douglas-fir stands in the climate protection scenario would further reduce seepage rates to 28 mm.
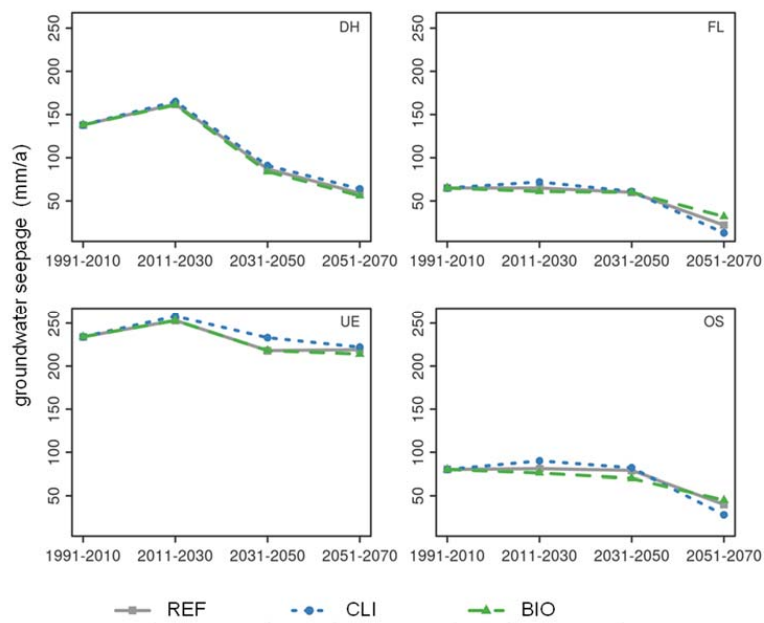
Figure 3. Simulated development of groundwater recharge in the four model regions: Diepholz (DH), Fläming (FL), Uelzen (UE), and Oder-Spree (OS) under the three silvicultural management scenarios: reference (REF), climate protection (CLI), and biodiversity (BIO) until 2070.

3.3. Element Budget Simulations

3.3.1. Regionalization of Carbon and Nitrogen Stocks and Base Saturation

The regionalization of C stocks was applied to measured data of the second NFSI in six federal states and yielded a good representation of the regional distribution of C stocks over large parts of the North German Lowland (Figure 4). Explained deviance of this soil C stock-GAM (SCS-GAM) was 80% ($r^2 = 0.83$), when applied to the second NFSI and 65% ($r^2 = 0.66$) for the first NFSI.
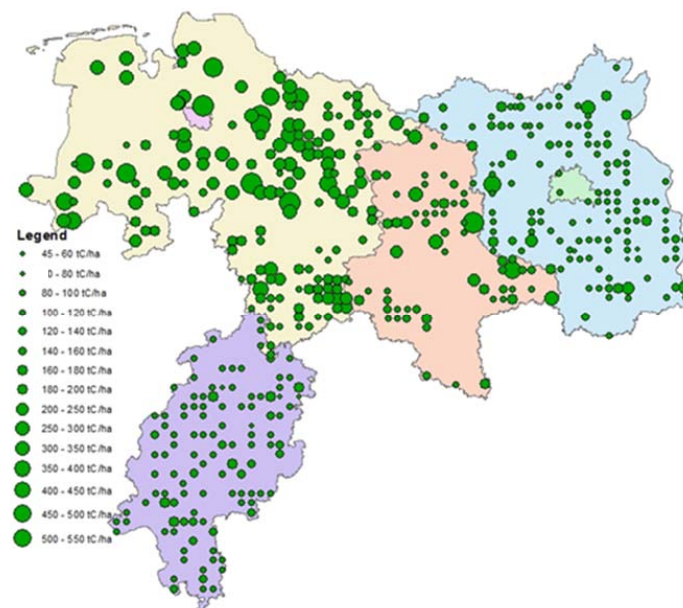

Figure 4. Carbon stocks of forest soils in and beyond the North German Lowland as regionalized with the SCS-GAM (Soil Carbon Stocks GAM) for the spatially representative plots of the second NFSI (federal states of Hesse, Lower Saxony, Bremen, Saxony-Anhalt, Brandenburg, and Berlin).

The SCS-GAM was also applied to derive C/N ratios at the same locations, employing the respective regionalization model for N stocks in combination. The N model explained 89% of the deviance in N stocks of the second NFSI ($r^2 = 0.86$) and 83% of their deviance in the first NFSI ($r^2 = 0.8$).

The base saturation model explained 73% of the variability in NFSI II data and 67% of their deviance, while it reached an r^2 of 0.71 (explained deviance of 74%) for data of the first NFSI.

3.3.2. Dynamic Simulation of Carbon Stocks

Based on NFSI data, the strongest shift in C stocks occurred in DH (annually $-2.8 \, \text{t C ha}^{-1}$), where organic soils prevail. In contrast, all three other model regions exhibited an increase in carbon stocks between 1991 and 2006 ($+0.1 \, \text{t ha}^{-1}$ to $+0.7 \, \text{t ha}^{-1}$). The C models Roth-C and YASSO07 both reflect this contrasting tendency in the amount of carbon stocks between DH and the other model regions (Figure 5). A quantitative evaluation reveals, however, that the Roth-C simulations match much better the observed C stocks that were regionalized from NFSI. Both models started with the initial C stocks of the first NFSI (1990) in each region. For the year 2007, YASSO07 overestimated C stocks in the model regions by +12%, +7%, +32%, and +57% (for DH, UE, FL, and OS, respectively), while the C stocks calculated with Roth-C deviated by -0.4%, -5%, $+2\%$, and -18% from the respective values for 2007. After about 2030, both models show a decreasing trend in C stocks that may partly be explained by increasing temperatures in the last 20 years of the simulation period, but also by reduced litter input due to a decrease in standing volume of the forest stands (cf. Figure 1).
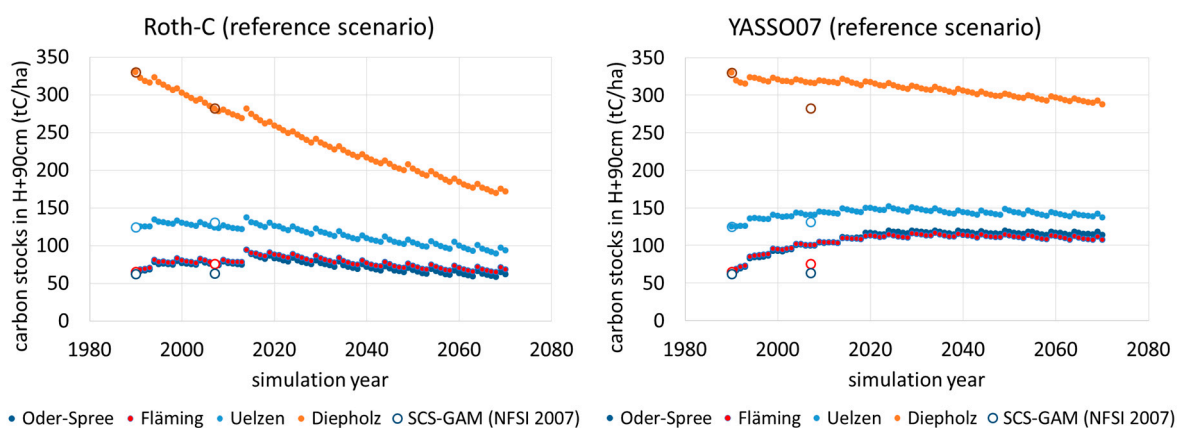

Figure 5. Development of soil carbon (C) stocks in the mineral soil up to 90 cm depth and the forest floor for the four model regions (only reference scenario) simulated with Roth-C (left) and YASSO07 (right). Statistically regionalized C stocks for both surveys of the NFSI are indicated as open circles in the color of each region.

3.3.3. Nitrogen Budget

1. Diepholz (DH)

The N budget of forests in DH is positive (inputs > outputs) under current (1991–2010) conditions and higher than in other model regions due to high N deposition and high N retention of forests on organic soils (Figure 6). The high soil organic matter stocks in DH are, however, increasingly reduced under the expected warmer conditions, such that the relation between slowly decreasing N depositions and increasing N losses shifts towards the side of N losses. In effect, the N budget is decreased to $-29.3 \, \text{kg ha}^{-1} \, \text{a}^{-1}$ until 2050–2070 in the reference scenario. The climate protection scenario intensifies this trend during the projection period of 60 years due to decreasing biomass volume. An attenuating effect is only expected in the last 20 years of the simulation period (2050–2070), when newly established forest stands achieve their maximum growth phase resulting in a slightly higher N budget of $-25.9 \, \text{kg ha}^{-1} \, \text{a}^{-1}$ as compared to the reference scenario. In contrast, accumulating

biomass in the biodiversity scenario provides a N sink that has a mitigating effect on the general trend of accelerating decomposition, resulting in a N budget of -22.8 kg ha^{-1} a^{-1} in 2050–2070.
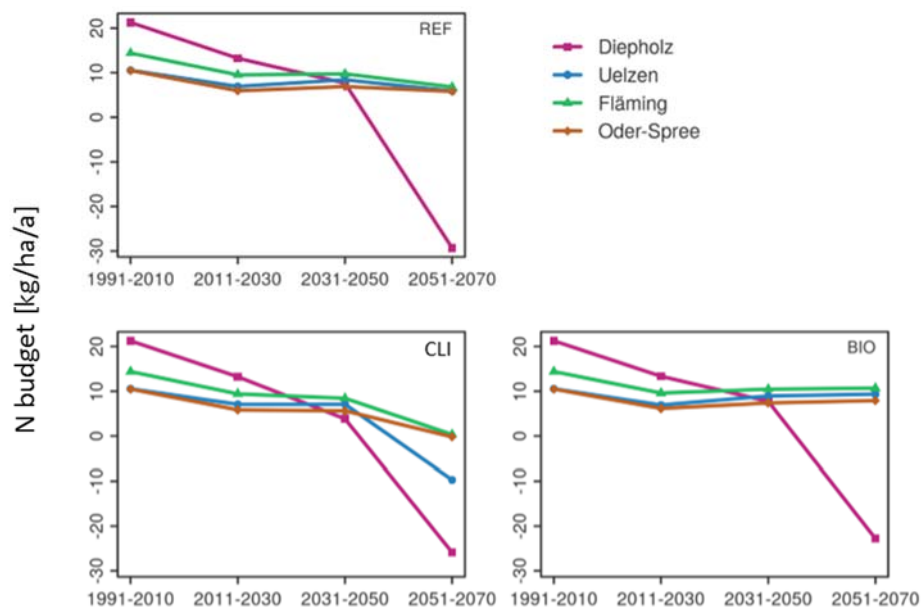

Figure 6. Simulated development of the nitrogen (N) budget in the four model regions under the three silvicultural management scenarios: reference (REF), climate protection (CLI), and biodiversity (BIO) until 2070.

2. Uelzen (UE)

In UE, at the beginning of the reference scenario simulation period, the forests may still partly retain N from the slowly decreasing N deposition that enables a N budget of $+10.5$ kg ha^{-1} a^{-1}. Nitrogen retention is also affected by a climate induced acceleration of decomposition, which decreases the N budget to 5.9 kg ha^{-1} a^{-1} in 2050–2070. In the climate protection scenario, the N budget is decreased by a high reduction of standing wood volume, resulting in a negative N budget of -9.7 kg ha^{-1} a^{-1} in 2050–2070. In the biodiversity scenario, tree biomass is accumulated in the period considered; thus, N is retained in the ecosystem, leading to a positive N budget of $+9.4$ kg ha^{-1} a^{-1} in 2050–2070.

3. Fläming (FL) and Oder-Spree (OS)

FL and OS show similar trends. An initially positive N budget is decreased due to an accelerated decomposition of soil organic matter under warmer conditions, resulting in a still positive, but lower N budget in the reference scenario in 2050–2070. In the climate protection scenario, the N budget decreases in both model regions to an almost balanced budget in 2050–2070, while the biodiversity scenario with the highest standing volume compared to the other scenarios enables a continuously positive N budget of 10.7 kg ha^{-1} a^{-1} in FL and 7.9 kg ha^{-1} a^{-1} in OS, respectively, in 2050–2070.

3.3.4. Nitrate in Seepage Water

Nitrate (NO_3^-) concentration increases continuously during the simulation period in all regions (Figure 7). The initially low NO_3^- concentrations in UE, FL and OS would increase until 2070 to values between 20 mg L^{-1} and 50 mg L^{-1}. In DH, where high N deposition occurs, even NO_3^- contents of 120 mg L^{-1} would be expected.
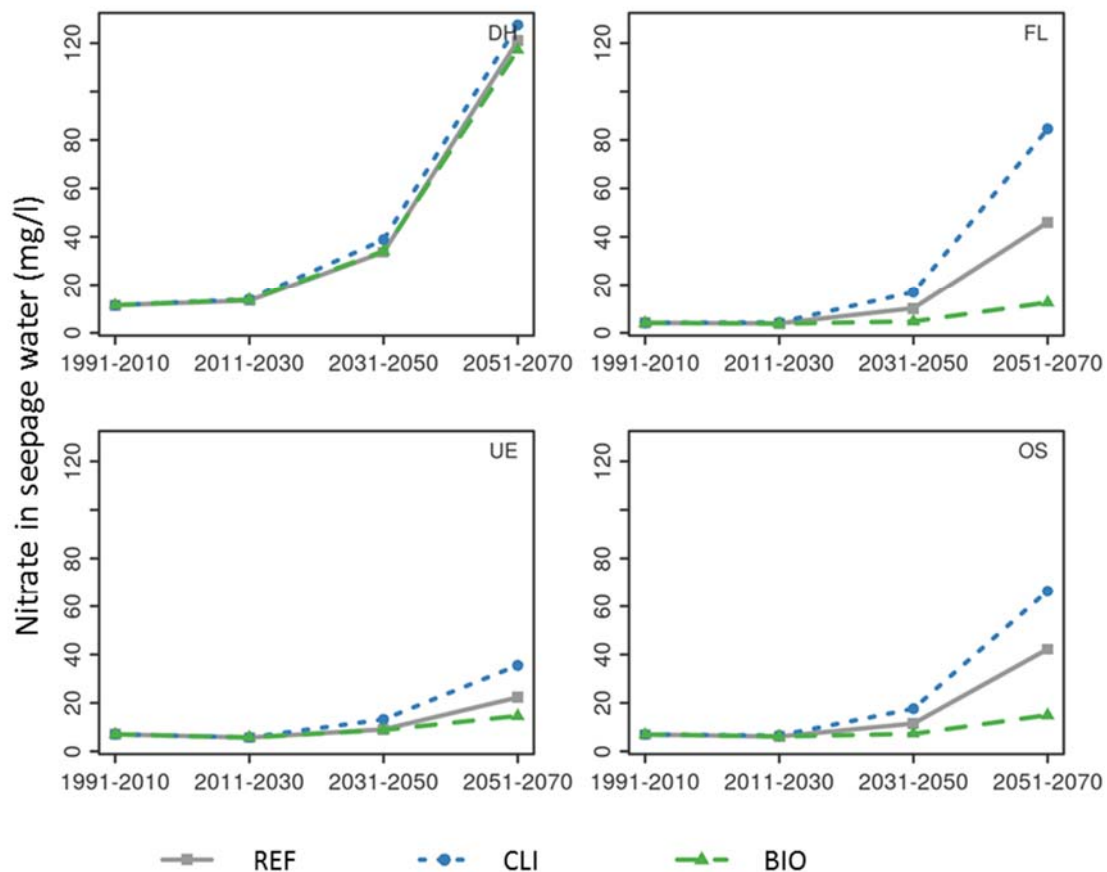
Figure 7. Simulated development of nitrate in seepage water in the four model regions: Diepholz (DH), Fläming (FL), Uelzen (UE), and Oder-Spree (OS) under the three silvicultural management scenarios: reference (REF), climate protection (CLI), and biodiversity (BIO) until 2070.

4. Discussion

4.1. Climate Projection

In general for climate change impact assessment, climate projections based on an ensemble approach are recommended. Ideally, different combinations of GCMs and regional climate models as well as several emission scenarios should be considered [33,85]. A simplified approach was chosen for our simulations. We based our impact assessment on the median run out of 21 different climate projections in order to avoid extreme scenarios. Our presented modelling approach is strongly driven by the climate projections of the Statistical Analogue Resampling Scheme (STARS) [36]. Wechsung and Wechsung [86,87] critically evaluated this approach. They quantified a negative precipitation bias of approx. 5% per 1 K temperature increase. Despite the model limitations, Wechsung and Wechsung [87] recommend STARS-based climate projections for vulnerability and uncertainty studies. For example, Bloch et al. [88] assessed the regional impact of drought events on the yield of legume-grass swards under STARS climate projections for the period 2062 to 2092 and derived conclusions for future management. In any case, a possible precipitation bias introduced by STARS should be taken into account when interpreting the results.

The climate projection used in this study, however, projects a slight increase of precipitation over 100 years. This increase would probably be higher, if STARS did not suffer from the potential bias. However, the precipitation trend obtained with the climate projection used in this study is within the range of precipitation changes produced by the application of different GCMs (-220 mm to $+218$ mm).

To obtain more robust estimations for decision support, the analysis of further climate and deposition scenarios is recommended.

4.2. Trends in Groundwater Recharge

The effect of the chosen climate projection on groundwater recharge can be inferred from the water budget simulations for NFSI plots (baseline scenario). Using observed forest stand and soil properties and assuming no change of these parameters, it shows how water budgets would evolve in a warmer climate, independent of changes introduced by forest management. Groundwater recharge under forests would be sharply reduced by 80 mm in DH, by 75 mm in UE, by 35 mm in FL, and by 50 mm in OS, which means most severe reductions in DH (-36%), FL (-39%) and OS (-50%), while the relative reduction is lowest in UE (-29%). Since precipitation does not change much in the climate scenario for DH, UE, and FL, the most important mechanisms leading to the reduction in water seepage rates is an increase in evaporative demand of the atmosphere due to rising temperature and an extension of the vegetation period, which increases losses due to evaporation and transpiration. The reduction is, however, higher, if precipitation is lowered additionally (OS and to some extent FL).

It is obvious, however, that todays' forest stands will evolve exhibiting other properties in the time period 2051–2070. The magnitude of the influence of evolving forest stands and better spatial representativeness may be judged by comparison with the water budget results for sampling points in the model regions. Here, groundwater recharge in the reference scenario would also be reduced, by 79 mm in DH, by 15 mm in UE, by 43 mm in FL, and by 40 mm in OS. Except for UE, the supra-regional pattern develops, thus, similar to a situation with actual stand properties. The much lower reduction of groundwater recharge rates in UE with evolving forests is not a consequence of the deviation in standing volume, since standing volume increases in this region, probably entailing an increased water consumption of the vegetation. However, it should be considered, that our modelling system does not account for the effects of increased atmospheric CO_2 concentration. On the one hand, an elevated atmospheric CO_2 concentration may increase photosynthesis, giving rise to forest growth; on the other hand, the water use efficiency is increased, resulting in a decreased transpiration [89].

The supra-regional pattern of groundwater recharge and the reductions until 2070 are mainly due to the climatic and regional differences among the model regions. The increasing evaporative demand of the atmosphere may best be fulfilled in DH, where soils with high field capacity or the access of the forest stands to groundwater facilitate the water uptake by vegetation and atmosphere, thereby strongly reducing the groundwater recharge by increased transpiration and evaporation. The sandy soils with low field capacity in UE, on the other hand, prevent a fulfillment of evaporative demand today as well as in the future; thus, the available soil water content is reduced, while groundwater recharge remains more or less constant. The low and lately decreasing precipitation in FL and OS is the main reason for lower groundwater recharge and higher reductions than in UE towards the end of the simulation period, which are most extreme in OS. The water deficit between evaporative demand and actual evaporation was also recently analyzed for Brandenburg using the A1B climate scenario regionalized with the WettReg model [90]. Similar to our study, the highest water deficits were found in OS, while the situation was less severe in FL.

The differences in groundwater recharge induced by the three forest management scenarios are small in all regions when compared to the impact of climate change. In DH, the biodiversity scenario leads to lower groundwater recharge due to higher evapotranspiration of the increasing standing volume in this scenario as compared to climate protection and reference. However, groundwater recharge rates in 2051–2070 deviate only by -5% and $+8\%$ for climate protection and biodiversity relative to the reference, respectively. Lower standing biomass is also the main reason in UE for the small difference between the climate protection (-2% relative to the reference scenario) and biodiversity scenario ($+1\%$). However, it is important to note that biomass accumulation under the biodiversity scenario is a temporary condition during the projection period considered. By delaying thinning and harvest operations due to increased target diameters and lower limits for allowable

cuts, the accumulated volume will, in parts, be exploited after 2070. This will partly compensate the higher groundwater recharge rates of the biodiversity scenario opposed to the other two management paths. In the period 2051 to 2070, the trend in standing volume in the biodiversity scenario in OS and FL is opposite to both other regions. A strong decrease in standing biomass is due to the aging of forest stands with lower transpiration rates. Though in these regions, standing biomass in the climate protection scenario is even lower, the forest stands in this scenario are in a younger and more productive stage with increasing proportions of Douglas-fir towards the end of the simulation period, leading to higher transpiration rates. The climate protection scenario, therefore, leads to lower groundwater recharge in these regions than the biodiversity scenario. It seems plausible that the differences in species conversion between the management scenarios will affect groundwater recharge in the long-term, i.e., well beyond the end of the considered projection period, and, therefore, confirm the advantageousness of the biodiversity scenario vs. the two others.

4.3. Trends in Soil Organic Matter

The amount of C stocks in the soil is the balance of organic matter input (mainly from root litter, foliar litter, and harvest residuals) and organic matter output by decomposition of organic substances, the products of which are emitted in the form of CO_2. For constant climatic and soil conditions, input and output approach an equilibrium after infinite time, where the amount of soil organic matter allows a decomposition rate that is equal to the average input of organic matter. The relevance of soils which are apart from the theoretical steady state of actual conditions and the consequences for soil C modelling are intensively discussed in [73]. The organic matter stocks in DH are obviously higher than expected under current climate, thereby allowing high decomposition rates that cannot be compensated by the vegetation's production of organic material, leading to decreasing C stocks. In contrast, soil organic matter stocks in the other regions are still increasing due to production being higher than decomposition until about 2030. After this point in time, however, decomposition seems to be higher than organic matter input and soil organic matter stocks will decrease under all considered management scenarios.

This is due to an increase of decomposition under a higher temperature and a decrease of litter input in those management scenarios and model regions which exhibit a reduced standing volume (cf. Figure 1).

On the one hand, decomposition rates are generally higher hence soil organic matter stocks lower in regions with a warmer climate. A comprehensive analysis of the global pattern of soil organic matter stocks has e.g., directly been used for the standard parameterization of YASSO07 [65] and similar empirical data were used to derive standard mineralization coefficients for Roth-C. Observed decomposition data show that a potential inhibition of decomposition under dry conditions is actually only realized in extremely arid regions, while decomposition rates across the whole of Europe are continuously rising the warmer it gets [65]. The stabilization of soil organic matter under dry conditions may, thus, only be locally important and does not reflect the decomposition rates of whole regions in Europe. Mineralization of soil organic matter is, however, still under discussion in recent literature [91–95]. Next to temperature, soil moisture as the other important driver for organic matter decomposition is explicitly taken into account by VSD+—a direct dependence of decomposition rates on soil moisture is modelled using the approach of [96], thereby overcoming limitations of the original Roth-C model.

On the other hand, a decrease in standing volume or biomass entails decreasing litter input which is the case in the reference scenario of all model regions except DH after 2050. Both, increasing decomposition and decreasing organic matter input cause the decrease in soil organic matter stocks.

As a consequence of the enhanced decomposition of soil organic matter and still high N soil retention, a decrease of the C/N ratio in the forest soil takes place (cf. [97]). Many studies show that the risk for elevated NO_3^- leaching increases with decreasing C/N ratio in regions with high N input [18,22,23,98].

The projected increase of N release results in a decrease of the N budget of forest soils in all model regions. Parallel to the decrease in soil organic matter, the climate protection scenario induces an even stronger decrease in tree biomass that additionally lowers the sink strength of the forest ecosystem for N. As a result, the supply of forest soils with new organic matter in the form of foliar and root litter is reduced and N budgets turn negative in all model regions. On the other hand, an increase in standing volume under the biodiversity scenario keeps NO_3^- concentrations low in three of the four model regions. In DH, the high N deposition and N release from soils with high organic matter stocks may not be compensated by the N uptake of the forest stands

Several studies showed that the C sequestration rate of forest soils is increased under elevated N deposition [99–101], however, the efficiency of this effect differs considerably [102,103]. It may to some extent be accounted for in the VSD+ simulations where the foliar N content is dependent on N deposition.

4.4. Trends in Nitrate Concentrations

The validation of simulated NO_3^- concentrations at single sampling locations is generally difficult due to the high variability of NO_3^- concentrations in seepage water [104–107]. Therefore, the simulated NO_3^- concentrations were compared for the first 20 years of the simulation (1991–2010) with independent large-scale NO_3^- observations in the surroundings of the model regions. The results of the comparison confirm the magnitude of the calculated values for each of the model regions (cf. [108] (Cloppenburg), [109] (Brandenburg), [110] (Mecklenburg-Vorpommern), [27] (North German Lowland)). A good coincidence was also found with NO_3^- concentrations that we derived from 1:2 extracts of the second NFSI in the model regions including 50 km surrounding area of each region (mean values DH: 5 mg/L, UE: 4 mg/L, FL: 6.9 mg/L, and very high coefficients of variation 101%, 212% and 185%, respectively). The concentrations of OS are given elsewhere [109]. The NO_3^- concentration at field capacity of the 1:2 extracts provides a solid basis for the estimation of NO_3^- losses with seepage water [111].

Uncertainties in the simulation of future NO_3^- concentrations arise from the representation of N uptake by the trees and from deposition. Considering the N concentration in the soil solution, the N uptake efficiency (Nupeff) is an essential parameter in the VSD+ model based on the assumption that forest ecosystems will usually lose some N, even in the case that N is the limiting nutrient. Uncertainties in regionalized and modelled N deposition especially concerning the dry deposition process and the underlying emission data are discussed elsewhere [112,113].

Gaseous emissions of N species due to denitrification are an alternative process that could lower NO_3^- concentrations in the soil. They were explicitly modelled in VSD+ as first-order processes depending on available N in soil solution after deposition, uptake, mineralisation and nitrification. An adjustment is made depending on soil pH. The uncertainty in the quantification of N emissions [114], especially for sandy soils [115], does not contradict observations revealing a generally rather small contribution of denitrification to the N budget [18].

Although the model system comprises many established and validated models, some of the models have high uncertainties in the parameterization (e.g., [116] for the VSD model). In combination with uncertainties in the input data, particularly with regard to climate projections, these uncertainties may counterbalance each other or accumulate along a cascade [117,118]. Consequently, further research to improve the input data as well as the impact models is necessary to reduce those uncertainties.

However, a future increase of NO_3^- concentrations in the model regions appears to be very likely because of the markedly reduced seepage flux in combination with accelerated turnover rates of N pools in soil organic matter. The results are a hint of the weakening capacity of forests to retain N [5,6]. Mellert et al. [111] postulate that N saturated Scots pine forest stands on sandy soils bear a high risk of elevated NO_3^- leaching due to the combination of highly permeable soils with high N stocks. When comparing the management scenarios, the climate protection scenario would aggravate the risk of NO_3^- leaching in the model regions during the projection period, while the biodiversity scenario

seems to have an extenuating effect. For FL and OS, NO_3^- concentrations in seepage water will exceed the limit of the WFD for groundwater according to model simulations in the period 2051–2070 under the climate protection and under the reference scenario. For DH, forest management seems to be of minor importance, since none of the management scenarios had a marked impact on the risk of enhanced NO_3^- leaching in this model region. Regardless of the assumed management scenario, NO_3^- concentrations in seepage water are expected to exceed the WFD limit in DH.

The effect of climate change on NO_3^- concentrations has been evaluated in other scientific studies as well. In a review of climate change effects on different land-use types [119], the included studies ranged from a limited increase to a possible doubling of NO_3^- concentrations by 2010. The authors expect an increase of N leaching in forests due to rising temperature. For a forested karst area, Dirnböck et al. [120] found positive as well as negative impacts of climate change on NO_3^- leaching from forest soils. Especially historical events (e.g., forest cutting) can have significant effects on the N cycle [24].

5. Conclusions

The relevance of NO_3^- leaching from forests in a warmer and slightly drier Central European climate is a matter of human health as well as ecosystem integrity that is not limited to the selected regions, since the mechanisms are the same in other regions as well. As forests are a main source of groundwater for drinking water abstraction, the legal threshold values of NO_3^- concentrations imposed by the WFD need to be applied in order to avoid a situation where a supra-regional trend towards increasing NO_3^- concentrations in drinking water increases health risks such as cyanosis or bowel cancer. On top of that, leached NO_3^- is also transferred to stream water, where it is a source of acidity and may substantially lower biodiversity. Since leached NO_3^- cannot leave the soil without cations, it is also a threat for soil fertility and forest health as it removes basic cations from the soil.

Despite the uncertainties in the estimation of NO_3^- concentrations in seepage water, a future increase in the model regions appears to be very likely due to a markedly reduced seepage flux. Due to the strong temperature increase, the increase in NO_3^- concentrations is even likely to be disproportionately higher, based on the expectation that higher decomposition of organic matter and lower C/N ratios aggravate the risk of NO_3^- leaching. Potential losses of gaseous N compounds due to denitrification could lower this risk while causing other problems with regard to greenhouse gases, but they are not expected. However, accurate quantification is extremely difficult due to numerous uncertainties in the model chain. Therefore, the appropriate forest management options for the special situation in the North German Lowland must be carefully chosen, since they may have a strong effect on the expected NO_3^- concentrations. The sink strength of forests for N should not be additionally lowered by overly strong reductions of standing biomass, since they are already at the limit of their N retention capacity.

The simulations indicate the high vulnerability of forests in the North German Lowland to climate change. The high amounts of organic matter stored in forest soils are susceptible to an increased decomposition in a warmer and slightly dryer climate. The probable combination of low seepage fluxes with increased decomposition of soil organic matter predisposes the investigated regions to higher NO_3^- concentrations in seepage water.

Author Contributions: S.F. analyzed the data, supported the element budget simulations, and wrote the paper; B.A. modelled the element budgets, supervised the model coupling, and wrote the paper; J.S. simulated the water budgets and wrote the paper, M.A. modelled forest development and wrote the paper, J.E. performed quality checks and edited the measurement data, and H.M. coordinated the research and wrote the paper.

Conflicts of Interest: The authors declare no conflict of interest. The founding sponsors had no role in the design of the study; in the collection, analyses, or interpretation of data; in the writing of the manuscript, and in the decision to publish the results.

Appendix A. Parameters Used in the VSD+ Model

Parameter	Description	Unit	Value/Source
SiteInfo	Site ID	-	consecutive number
period	starting and ending time of simulation	y y	1990 2070
thick	thickness of the soil compartment	m	0.9
bulkdens	bulk density of the soil	g/cm^3	digital soil map (chapter 2.5)
Clay_ct	clay content of the soil	%	digital soil map (chapter 2.5)
Theta	water content of the soil	m^3/m^3	WaSiM-ETH (chapter 2.4)
pCO2fac	CO_2 pressure in soil solution (multiple of pCO_2 [atm] in air)	-	[67]
CEC	cation exchange capacity	meq/kg	digital soil map (chapter 2.5)
bsat_0	initial base saturation	-	generalized additive model (chapter 2.5)
ECa_0	initial Ca saturation	-	−1: determined by the model
EMg_0	initial Mg saturation	-	−1: determined by 'the model
EK_0	initial K saturation	-	−1: determined by the model
Excmod	cation exchange model option (1 = Gaines-Thomas; 2 = Gapon)	-	1
lgKAlBC	log10 of selectivity constant for Al-Bc exchange	eq/m^3	[78]
lgKHBC	log10 of selectivity constant for H-Bc exchange	eq/m^3	[78]
expAl	exponent (>0) in [Al] = KAlox [H] expel	-	[78]
lgKAlox	log10 of gibbsite equilibrium constant	$((mol/L)^{1-expAl})$	[78]
Cpool_0	initial amount of C in soil (per unit area)	g/m^2	generalized additive model (chapter 2.5)
CNrat_0	initial C:N ratio insoil	g/g	generalized additive model (chapter 2.5)
RCOOmod	organic acid model: 0 = Oliver, 1 = mono-protic	-	0
RCOOpars	1 or 3 parameters for organic dissociation model	-	a: 0.96; b: 0.9; c: −0.039
cRCOO	total concentration of organic acids (m*DOC)	mol/m^3	0.004379
TempC	average soil temperature	°C	see chapter 2.2
percol	percolation (precipitation surplus)	m/a	WaSiM-ETH (chapter 2.4)
Ca_we	weathering rate of Ca	$eq/m^3/a$	regression model based on PROFILE [121] simulations [122]
Mg_we	weathering rate of Mg	$eq/m^3/a$	regression model based on PROFILE [121] simulations [122]
K_we	weathering rate of K	$eq/m^3/a$	regression model based on PROFILE [121] simulations [122]
Na_we	weathering rate of Na	$eq/m^3/a$	regression model based on PROFILE [121] simulations [122]
SO2_dep	deposition of SO2	$eq/m^2/a$	see chapter 2.5
NOx_dep	deposition of NOx	$eq/m^2/a$	see chapter 2.5
NH3_dep	deposition of NH3	$eq/m^2/a$	see chapter 2.5
Ca_dep	deposition of Ca	$eq/m^2/a$	see chapter 2.5
Mg_dep	deposition of Mg	$eq/m^2/a$	see chapter 2.5
K_dep	deposition of K	$eq/m^2/a$	see chapter 2.5
Na_dep	deposition of Na	$eq/m^2/a$	see chapter 2.5
Cl_dep	deposition of Cl	$eq/m^2/a$	see chapter 2.5
kdenit	maximum denitrification rate	a^{-1}	4
Nfix	N fixation	$eq/m^2/a$	0
Nupeff	Uptake efficiency of available N (0-1)	-	0.96–0.99 see documentation and discussion
rf_miR	modifying factor of mineralization due to moisture and temperature for the RothC C/N model	-	MetHyd functions [123] coupled with WaSiM-ETH
rf_nit	modifying factor of nitrification due to moisture and temperature	-	MetHyd functions [123] coupled with WaSiM-ETH
rf_denit	modifying factor of denitrification due to moisture and temperature	-	MetHyd functions [123] coupled with WaSiM-ETH
N_gupt	Total annual removal (uptake) of N from the soil by the vegetation	$eq/m^2/a$	chapter 2.4
Ca_upt	Net annual removal (uptake) of Ca from the soil by the vegetation	$eq/m^2/a$	chapter 2.4
Mg_upt	Net annual removal (uptake) of Mg from the soil by the vegetation	$eq/m^2/a$	chapter 2.4
K_upt	Net annual removal (uptake) of K from the soil by the vegetation	$eq/m^2/a$	chapter 2.4
P_upt	Net annual removal (uptake) of P from the soil by the vegetation	$eq/m^2/a$	chapter 2.4
Clf	C litterfall flux	$g/m^2/a$	chapter 2.4
Nlf	N litterfall flux	$g/m^2/a$	chapter 2.4
QIlf	Quality index of litterfall (-) for the RothC model	0.25	default value valid for forests

Appendix B. Available NFSI-Parameters for the Development of GAMs

The use of parameters for the parameter selection process and their availability for different points in time (NFSI I, NFSI II) and soil depths is given, the headlines meaning the mineral soil up to 90 cm depth (M90), the mineral soil up to 140 cm depth (M140), the mineral soil up to 90 cm depth plus a humus layer (M90+), and the mineral soil up to 140 cm depth plus a humus layer (M140+).

Parameter	Unit	NFSI I	NFSI II	M 90	M 140	M90+	M140+
Federal State	-	✓	✓				
Ownership	-	✓	✓				
Forest authority	-	✓	✓				
County	-	✓	✓				
Growth zone	-	✓	✓				
Growth district	-	✓	✓				
Soil landscape	-	✓	✓				
Soil region	-	✓	✓				
Easting	m	✓	✓				
Northing	m	✓	✓				
Height above sea level	m	✓	✓				
Slope	-	✓	✓				
Exposition	-	✓	✓				
Form of relief	-	✓	✓				
Situation in relief	-	✓	✓				
Number of liming events	number	✓	✓				
Amount of lime applied	t/ha	✓	✓				
Liming per aera and year	number/ha/a	✓	✓				
Year of last liming	a	✓	✓				
Trophic level	-	✓	✓				
Degree of podzolization	-	✓	✓				
Forest Type (Species)	-		✓				
coarse fragments	%	✓	✓	✓	✓		
Potential CEC	cmolc/kg, cmolc/ha	✓	✓	✓	✓		
pH (KCl)	log [H$^+$]	✓	✓	✓	✓	✓	✓
Effective CEC	molc/kg, molc/ha	✓	✓	✓	✓	✓	✓
Carbon stocks	kg/ha	✓	✓	✓			
Base saturation	%	✓	✓	✓	✓		
C/N-ratio	-	✓	✓	✓	✓	✓	✓
Carbonate	Yes/No	✓	✓	✓	✓	✓	✓
Actual water level	cm		✓				
Substrate group	-		✓				
Bedrock type	-		✓				
Type of loose material	-		✓				
Annual precipition	mm	✓	✓				
Avg. temperature	°C	✓	✓				
Soil type	-	✓	✓				
Soil class	-	✓	✓				
Hydromorphology	Yes/No	✓	✓				
Forest Type	Conifer/broad/mix	✓					
N-deposition (4 years mean)	eq/ha/a	✓	✓				
S-deposition (4 years mean)	eq/ha/a	✓	✓				
Sand	%		✓	✓	✓		
Silt	%		✓	✓	✓		
Clay	%		✓	✓	✓		
Weathering surface	m^2/ha		✓	✓	✓		
Fine soil	t/ha	✓	✓	✓		✓	
N-stocks	kg/ha		✓	✓			
Precipitation in winter	mm		✓				
Temperature in winter	°C		✓				
Precipitation in summer	mm		✓				
Temperature in summer	°C		✓				
Eff. Field capacity	%		✓	✓			
Main rooting depth	cm		✓				
Rooting depth fine roots	cm		✓				
Rooting depth coarse roots	cm		✓				
Ca^{2+}-excange. capacity	kg/ha		✓	✓		✓	
K$^+$-excange. capacity	kg/ha		✓	✓		✓	
Mg^{2+}-excange. capacity	kg/ha		✓	✓		✓	
Thickness of humus layer	cm		✓				
Humus type	-	✓	✓				

References

1. Spiecker, H. Overview of recent growth trends in European forests. *Water Air Soil Pollut.* **1999**, *116*, 33–46. [CrossRef]
2. Vitousek, P.M.; Howarth, R.W. Nitrogen limitation on land and in the sea: How can it occur? *Biogeochemistry* **1991**, *13*, 87–115. [CrossRef]
3. Waldner, P.; Thimonier, A.; Graf Pannatier, E.; Etzold, S.; Schmitt, M.; Marchetto, A.; Rautio, P.; Derome, K.; Nieminen, T.M.; Nevalainen, S.; et al. Exceedance of critical loads and of critical limits impacts tree nutrition across Europe. *Ann. For. Sci.* **2015**, *72*, 929–939. [CrossRef]
4. Laubhann, D.; Sterba, H.; Reinds, G.J.; de Vries, W. The impact of atmospheric deposition and climate on forest growth in European monitoring plots: An individual tree growth model. *For. Ecol. Manag.* **2009**, *258*, 1751–1761. [CrossRef]
5. Aber, J.D.; McDowell, W.; Nadelhoffer, K.J.; Magill, A.; Berntson, G.; Kamakea, M.; McNulty, S.; Currie, W.; Rustad, L.; Fernandez, I. Nitrogen saturation in temperate forest ecosystems: Hypotheses revisited. *BioScience* **1998**, *48*, 921–934. [CrossRef]
6. Aber, J.D.; Nadelhoffer, K.J.; Steudler, P.; Melillo, J.M. Nitrogen saturation in northern forest ecosystems. *BioScience* **1989**, *39*, 378–386. [CrossRef]
7. Erisman, J.W.; Dammers, E.; van Damme, M.; Soudzilovskaia, N.; Schaap, M. Trends in EU nitrogen deposition and effects on ecosystems. *Air Waste Manag. Assoc. Mag.* **2015**, *65*, 31–35.
8. Oulehle, F.; Cosby, B.J.; Austnes, K.; Evans, C.D.; Hruska, J.; Kopácek, J.; Moldan, F.; Wright, R.F. Modelling inorganic nitrogen in runoff: Seasonal dynamics at four European catchments as simulated by the MAGIC model. *Sci. Total Environ.* **2015**, *536*, 1019–1028. [CrossRef] [PubMed]
9. De Vries, W.; Dobbertin, M.H.; Solberg, S.; van Dobben, H.F.; Schaub, M. Impacts of acid deposition, ozone exposure and weather conditions on forest ecosystems in Erurope: An overview. *Plant Soil* **2014**, *380*, 1–45. [CrossRef]
10. Reuss, J.O.; Johnson, D.W. *Acid Deposition and the Acidification of Soils and Waters*; Ecol. Studies 59; Springer: New York, NY, USA, 1986; 120p.
11. Vitousek, P.M.; Aber, J.D.; Howarth, R.W.; Likens, G.E.; Matson, P.A.; Schindler, D.W.; Schlesinger, W.H.; Tilman, G.D. Human alteration of the global nitrogen cycle: Causes and consequences. *Ecol. Appl.* **1997**, *7*, 737–750.
12. Waldner, P.; Marchetto, A.; Thimonier, A.; Schmitt, M.; Rogora, M.; Granke, O.; Mues, V.; Hansen, K.; Karlsson, G.P.; Zlindra, D.; et al. Detection of temporal trends in atmospheric deposition of inorganic nitrogen and sulphate to forests in Europe. *Atmos. Environ.* **2014**, *95*, 363–374. [CrossRef]
13. Meesenburg, H.; Ahrends, B.; Fleck, S.; Wagner, M.; Fortmann, H.; Scheler, B.; Klinck, U.; Dammann, I.; Eichhorn, J.; Mindrup, M.; et al. Long-term changes of ecosystem services at Solling, Germany: Recovery from acidification, but increasing nitrogen saturation? *Ecol. Indic.* **2016**, *65*, 103–112. [CrossRef]
14. Ahrends, B.; Meesenburg, H.; Döring, C.; Jansen, M. A Spatio-Temporal Modelling Approach for Assessment of Management Effects in forest catchments. In *Status and Perspectives of Hydrology in Small Basin*; International Association of Hydrological Sciences: Wallingford, UK, 2010; pp. 32–37.
15. Von Der Heide, C.; Böttcher, J.; Deurer, M.; Weymann, D.; Well, R.; Duijnisveld, W.H.M. Spatial variability of N_2O concentrations and of denitrification-related factors in the surficial groundwater of a catchment in Northern Germany. *J. Hydrol.* **2008**, *360*, 230–241. [CrossRef]
16. EU Directive 2000/60/EC of the European Parliament and of the Council of 23 October 2000 Establishing a Framework for Community Action in the Field of Water Policy. *Off. J. Eur. Commun.* **2000**, *43*, 1–72.
17. EU Directive 2006/118/EC of the European Parliament and of the Council of 12 December 2006 on the Protection of Groundwater against Pollution and Deterioration. *Off. J. Eur. Commun.* **2006**, *49*, 19–31.
18. Borken, W.; Matzner, E. Nitrate leaching in forest soils: An analysis of long-term monitoring sites in Germany. *J. Plant Nutr. Soil Sci.* **2004**, *167*, 277–283. [CrossRef]
19. Lovett, G.M.; Goodale, C.L. A New Conceptual Model of Nitrogen Saturation Based on Experimental Nitrogen Addition to an Oak Forest. *Ecosystems* **2011**, *14*, 615–631. [CrossRef]
20. Gundersen, P.; Schmidt, I.K.; Raulund-Rasmussen, K. Leaching of nitrate from temperate forests—Effects of air pollution and forest management. *Environ. Rev.* **2006**, *14*, 1–57. [CrossRef]

21. Prietzel, J.; Kaiser, K.O. De-eutrophication of a nitrogen-saturated Scots pine forest by prescribed litter-raking. *J. Plant Nutr. Soil Sci.* **2005**, *168*, 461–471. [CrossRef]

22. Dise, N.B.; Matzner, E.; Forsius, M. Evaluation of organic horizon C/N ratio as an indicator of nitrate leaching in conifer forests across Europe. *Environ. Pollut.* **1998**, *102*, 453–456. [CrossRef]

23. Gundersen, P.; Callesen, I.; De Vries, W. Nitrate leaching in forest ecosystems is related to forest floor C/N ratios. *Environ. Pollut.* **1998**, *102*, 403–407. [CrossRef]

24. Bernal, S.; Hedin, L.O.; Likens, G.E.; Gerber, S.; Buso, D.C. Complex response of the forest nitrogen cycle to climate change. *Proc. Natl. Acad. Sci. USA* **2012**, *109*, 3406–3411. [CrossRef] [PubMed]

25. *IPCC Climate Change 2014: Synthesis Report*; Contribution of Working Groups I, II and III to the Fifth Assessment Report of the Intergovernmental Panel on Climate Change; Core Writing Team; Pachauri, R.K., Meyer, L.A., Eds.; IPCC: Geneva, Switzerland, 2014; 151p.

26. Collins, M.; Knutti, R.; Arblaster, J.; Dufresne, J.-L.; Fichefet, T.; Friedlingstein, P.; Gao, X.; Gutowski, W.; Johns, T.; Krinner, G.; et al. Long-term climate change: Projections, commitments and irreversibility. In *Climate Change 2013: The Physical Science Basis*; Contribution of Working Group I to the Fifth Assessment Report of the Intergovernmental Panel on Climate Change; Stocker, T., Qin, D., Plattner, G.-K., Tignor, M., Allen, S., Doschung, J., Nauels, A., Xia, Y., Bex, V., Midgley, P., Eds.; Cambridge University: Cambridge, UK, 2013; pp. 1029–1136.

27. Kiese, R.; Heinzeller, C.; Werner, C.; Wochele, S.; Grote, R.; Butterbach-Bahl, K. Quantification of nitrate leaching from German forest ecosystems by use of a process oriented biogeochemical model. *Environ. Pollut.* **2011**, *159*, 3204–3214. [CrossRef] [PubMed]

28. Wade, A.J.; Durand, P.; Beaujouan, V.; Wessel, W.W.; Raat, K.J.; Whitehead, P.G.; Butterfield, D.; Rankinen, K.; Lepisto, A. A nitrogen model for European catchments: INCA, new model structure and equations. *Hydrol. Earth Syst. Sci.* **2002**, *6*, 559–582. [CrossRef]

29. Thiele, J.C.; Nuske, R.; Ahrends, B.; Panferov, O.; Albert, M.; Staupendahl, K.; Junghans, U.; Jansen, M.; Saborowski, J. Climate change impact assessment—A simulation experiment with Norway spruce for a forest district in Central Europe. *Ecol. Model.* **2017**, *346*, 30–47. [CrossRef]

30. Albert, M.; Hansen, J.; Nagel, J.; Schmidt, M.; Spellmann, H. Assessing risks and uncertainties in forest dynamics under different management scenarios and climate change. *For. Ecosyst.* **2015**, *2*, 14. [CrossRef]

31. Albert, M.; Leefken, G.; Nuske, R.S.; Ahrends, B.; Sutmöller, J.; Spellmann, H. Auswirkungen von klimatischer Unsicherheit auf die Forstplanung am Beispiel von vier Regionen im norddeutschen Tiefland. *Allgemeine Forst und Jagdzeitung* **2016**, *187*, 161–184.

32. Messal, H.; Debebe, W.; Fohrer, N. Raum-zeitliche Analyse von Abfluss, Nährstoffen und physikalisch-chemischer Eigenschaften in Flusseinzugsgebieten des Norddeutschen Tieflandes. *Forum für Hydrologie und Wasserbewirtschaftung* **2015**, *35*, 1–10.

33. Moss, R.; Babiker, M.; Brinkmann, S.; Calvo, E.; Carter, T.R.; Edmonds, J.; Elgizouli, I.; Emori, S.; Erda, L.; Hibbard, K.; et al. *Towards New Scenarios for Analysis of Emissions, Climate Change, Impacts, and Response Strategies*; Intergovernmental Panel on Climate Change, Geneva, Technical Summary; Intergovernmental Panel on Climate Change: Geneva, Switzerland, 2008; 25p.

34. Van Vuuren, D.P.; Edmonds, J.; Ksinuma, M.; Riahl, K.; Thomson, A.; Hibbard, K.; Hurtt, G.C.; Kram, T.; Krey, V.; Lamarque, J.-F.; et al. The representative concentration pathways: An overview. *Clim. Chang.* **2011**, *109*, 5–31. [CrossRef]

35. Stevens, B.; Giorgetta, M.; Esch, M.; Mauritsen, T.; Crueger, T.; Rast, S.; Salzmann, M.; Schmidt, H.; Bader, J.; Block, K.; et al. Atmospheric component of the MPI-M Earth System Model: ECHAM6. *J. Adv. Model. Earth Syst.* **2013**, *5*, 146–172. [CrossRef]

36. Orlowsky, B.; Gerstengarbe, F.-W.; Werner, P.C. A resampling scheme for regional climate simulations and its performance compared to a dynamical RCM. *Theor. Appl. Climatol.* **2008**, *92*, 209–223. [CrossRef]

37. Schulla, J. *Model Description Wasim Completely Revised Version of 2012 with 2013 to 2015 Extensions*; Technical Report; Hydrology Software Consulting J. Schulla: Zürich, Switzerland, 2015; p. 332.

38. Gerstengabe, F.W.; Werner, P.C.; Österle, H.; Burghoff, O. Winter storm- and summer thunderstorm-related loss events with regard to climate change in Germany. *Theor. Appl. Climatol.* **2013**, *114*, 715–724. [CrossRef]

39. NMLELV—Niedersächsisches Ministerium für den Ländlichen Raum, Ernährung, Landwirtschaft und Verbraucherschutz (Ed.) *Langfristige ökologische Waldentwicklung. Richtlinie zur Baumartenwahl. Aus dem Walde-Schriftenreihe Waldentwicklung Niedersachsen 54*; Niedersächsisches Forstplanungsamt: Wolfenbüttel, Germany, 2004.

40. Sutmöller, J.; Hentschel, S.; Hansen, J.; Meesenburg, H. Coupled forest growth-hydrology modelling as an instrument for the assessment of effects of forest management on hydrology in forested catchments. *Adv. Geosci.* **2011**, *27*, 149–154. [CrossRef]

41. Hansen, J.; Nagel, J. *Waldwachstumskundliche Softwaresysteme auf Basis von TreeGrOSS—Anwendungen und theoretische Grundlagen*; Beiträge aus der NW-FVA 11; Nordwestdeutsche Forstliche Versuchsanstalt: Göttingen, Germany, 2014; 224p.

42. Schmidt, M. Ein longitudinales Höhen-Durchmesser Modell für Fichte in Deutschland. In *Tagungsband der 21. Jahrestagung der Sektion Forstliche Biometrie und Informatik im DVFFA*; Department Ecoinformatics, Biometrics and Forest Growth, Büsgeninstitut Georg-August University of Göttingen: Tharandt, Germany, 2009; pp. 97–120.

43. Lappi, J. Calibration of height and volume equations with random parameters. *For. Sci.* **1991**, *37*, 781–801.

44. Menzel, A. *Phänologie von Waldbäumen unter sich ändernden Klimabedingungen-Auswertung der Beobachtungen in den Internationalen Phänologischen Gärten und Möglichkeiten der Modellierung von Phänodaten*; Forstliche Forschungsberichte München 164; Forstwissenschaftliche Fakultät der Universität München and Bayerische Landesanstalt für Wald und Forstwirtschaft: Freising, Germany, 1997; p. 147.

45. Wilpert, K.V. *Die Jahrringstruktur von Fichten in Abhängigkeit vom Bodenwasserhaushalt auf Pseudogley und Parabraunerde. Ein Methodenkonzept zur Erfassung Standortsspezifischer Wasserstreßdisposition*; Freiburger Bodenkundliche Abhandlungen, Institut für Bodenkunde und Waldernährungslehre, University of Freiburg: Freiburg, Germany, 1990.

46. Walther, A.; Linderholm, H.W. A comparison of growing season indices for the Greater Baltic Area. *Int. J. Biometeorol.* **2006**, *51*, 107–118. [CrossRef] [PubMed]

47. Frich, P.; Alexander, L.V.; Della-Marta, P.; Gleason, B.; Haylock, M.; Klein Tank, A.M.G.; Peterson, T. Observed coherent changes in climatic extremes during the second half of the twentieth century. *Clim. Res.* **2002**, *19*, 193–212. [CrossRef]

48. Hammel, K.; Kennel, M. *Charakterisierung und Analyse der Wasserverfügbarkeit und des Wasserhaushalts von Waldstandorten in Bayern mit dem Simulationsmodell BROOK90*; Forstliche Forschungsberichte München 185; Heinrich Frank: München, Germany, 2001; 148p.

49. Bonten, L.; Mol-Diijkstra, J.P.; Wiegger, R.; Reinds, G.J. *GrowUp: A Tool for Computing Forest Growth, Nutrient Uptake and Litterfall*; CCE Status Report: Modelling and Mapping of Atmospherically-induced Ecosystem Impacts in Europe Coordination Centre for Effects; RIVM: Bilthoven, The Netherlands, 2012; pp. 43–47.

50. Jacobsen, C.; Rademacher, P.; Meesenburg, H.; Meiwes, K.J. Gehalte chemischer Elemente in Baumkompartimenten-Literaturstudie und Datensammlung. *Berichte des Forschungszentrums Waldökosysteme Reihe B* **2003**, *69*, 81.

51. Van Genuchten, M.T. A closed form equation for predicting the hydraulic conductivity of unsaturated soils. *Soil Sci. Soc. Am. J.* **1980**, *44*, 892–898. [CrossRef]

52. Richter, A.; Adler, G.H.; Fahrak, M.; Eckelmann, W. *Erläuterungen zur Nutzungsdifferenzierten Bodenübersichtskarte der Bundesrepublik Deutschland im Maßstab 1:1.000,000 (BÜK 1000 N, Version 2.3)*; Bundesanstalt für Geowissenschaften und Rohstoffe (BGR): Hannover, Germany, 2007; 53p.

53. Wessolek, G.; Kaupenjohann, M.; Renger, M. *Bodenphysikalische Kennwerte und Berechnungsverfahren für die Praxis*; Bodenökologie und Bodengenese; Technische Universität Berlin: Berlin, Germany, 2009; 80p.

54. Zeng, M.; De Vries, W.; Bonten, L.T.C.; Zhu, Q.; Hao, T.; Liu, X.; Xu, M.; Shi, X.; Zhang, F.; Shen, J. Model-Based Analysis of the Long-Term Effects of Fertilization Management on Cropland Soil Acidification. *Environ. Sci. Technol.* **2017**, *51*, 3843–3851. [CrossRef] [PubMed]

55. Posch, M.; Reinds, G.J. A very simple dynamic soil acidification model for scenario analyses and target load calculations. *Environ. Model. Softw.* **2009**, *24*, 329–340. [CrossRef]

56. Gauger, T.; Haenel, H.-D.; Rösemann, C.; Nagel, H.-D.; Becker, R.; Kraft, P.; Schlutow, A.; Schütze, G.; Weigelt-Kirchner, R.; Anshelm, F. *Nationale Umsetzung UNECE-Luftreinhaltekonvention (Wirkung)*; Abschlussbericht zum UFOPLAN-Vorhaben FKZ 204 63 252; Umweltbundesamt: Dessau-Rosslau, Germany, 2008.

57. Ahner, J.; Ahrends, B.; Engel, F.; Hansen, J.; Hentschel, S.; Hurling, R.; Meesenburg, H.; Mestermacher, U.; Meyer, P.; Möhring, B.; et al. *Waldentwicklungsszenarien für das Hessische Ried*; Entscheidungsunterstützung vor dem Hintergrund sich beschleunigt ändernder Wasserhaushalts- und Klimabedingungen und den Anforderungen aus dem europäischen Schutzgebietssystem Natura 2000; Beiträge aus der Nordwestdeutschen Forstlichen Versuchsanstalt, Nordwestdeutsche Forstliche Versuchsanstalt: Göttingen, Germany, 2013; 398p.

58. Cakmak, D.; Beloica, J.; Perovic, V.; Kadovic, R.; Mrvic, V.; Knezevic, J.; Belanovic, S. Atmospheric deposition effects on agricultural soil acidification state—Key study: Krupanj municipality. *Arch. Environ. Prot.* **2015**, *40*, 137–148.

59. Pecka, T.; Mill, W. Modelling of atmospheric nitrogen deposition effects to polish terrestrial ecosystems for various emission scenarios until the target year 2020. *Environ. Prot. Eng.* **2012**, *38*, 133–143.

60. Rowe, E.C.; Tipping, E.; Posch, M.; Oulehle, F.; Cooper, D.M.; Jones, T.G.; Burden, A.; Hall, J.; Evans, C.D. Predicting nitrogen and acidity effects on long-term dynamics of dissolved organic matter. *Environ. Pollut.* **2014**, *184*, 271–282. [CrossRef] [PubMed]

61. Bonten, L.T.C.; Reinds, G.J.; Posch, M. A model to calculate effects of atmospheric deposition on soil acidification, eutrophication and carbon sequestration. *Environ. Model. Softw.* **2016**, *79*, 75–84. [CrossRef]

62. Bonten, L.; Posch, M.; Reinds, G.J. *The VSD+ Soil Acidification Model. Model Description and User Manual Version 0.20*; Alterra: Wageningen, Germany, 2011; 19p.

63. Mol-Dijkstra, J.P.; Reinds, G.J. *Technical Documentation of the Soil Model VSD+, Status A*; WOT-Technical Report 88, Statutory Research Tasks Unit for Nature & the Environment (WOT Natuur & Milieu); Wageningen University and Research: Wageningen, The Netherlands, 2017; p. 88.

64. Coleman, K.; Jenkinson, D.S. RothC-26.3. In *Evaluation of Soil Organic Matter Modells Using Existing Long-Term Data Sets*; Powlson, D.S., Smith, P., Smith, J.U., Eds.; Springer: Berlin/Heidelberg, Germany; New York, NY, USA, 1996; pp. 237–246.

65. Tuomi, M.; Thum, T.; Järvinen, H.; Fronzek, S.; Berg, B.; Harmon, M.; Trofymow, J.A.; Sevanto, S.; Liski, J. Leaf litter decomposition—Estimates of global variability based on Yasso07 model. *Ecol. Model.* **2009**, *220*, 3362–3371. [CrossRef]

66. De Vries, W.; Hettelingh, J.-P.; Posch, M. *Critical Loads and Dynamic Risk Assessments*; Environmental Pollution, 25; Springer: Dordrecht, The Netherlands; Heidelberg, Germany; New York, NY, USA; London, UK, 2015; pp. 171–205. 647p.

67. Schelhaas, M.J.; Eggers, J.; Lindner, M.; Nabuurs, G.J.; Pussinen, A.; Paivinen, R.; Schuck, A.; Verkerk, P.J.; Van Der Werf, D.C.; Zudin, S.L. *Model Documentation for the European Forest Information Scenario Model (EFISCEN 3.1.3)*; Alterra Report 1559, EFI Technical Report 26; Alterra: Wageningen, The Netherlands, 2007; 119p.

68. Kane, E.S.; Betts, E.F.; Burgin, J.J.; Clilverd, H.M.; Crenshaw, C.L.; Fellman, J.B.; Myers-Smith, I.H.; O'Donnel, J.A.; Sobota, D.J.; Van Verseveld, W.J.; et al. Precipitation control over inorganic nitrogen import-export budgets across watersheds: A synthesis of long-term ecological research. *Ecohydrology* **2008**, *1*, 105–117. [CrossRef]

69. Riek, W.; Wolff, B. Standörtliche Rahmenbedingungen für den Umbau von Waldbeständen im nordostdeutschen Tiefland–Ergebnisse der BZE. In *Eberswalder Wissenschaftliche Schriften*; Deutscher Landwirtschaftsverlag: Berlin, Germany, 1999; pp. 173–178.

70. Wellbrock, N.; Aydin, C.T.; Block, J.; Bussian, B.; Deckert, M.; Diekmann, O.; Evers, J.; Fetzer, K.D.; Gauer, J.; Gehrmann, J.; et al. *Bodenzustandserhebung im Wald (BZE II), Arbeitsanleitung für die Außenaufnahmen*; Bundesministerium für Ernährung, Landwirtschaft und Verbraucherschutz: Bonn, Germany, 2006; 431p.

71. Falloon, P.; Smith, P.; Coleman, K.; Marshall, S. Estimating the size of the inert organic matter pool for use in the Rothamsted carbon model. *Soil Biol. Biochem.* **1998**, *30*, 1207–1211. [CrossRef]

72. Dalsgaard, L.; Astrup, R.; Antón-Fernández, C.; Borgen, S.K.; Breidenbach, J.; Lange, H.; Lehtonen, A.; Liski, J. Modeling Soil Carbon Dynamics in Northern Forests: Effects of Spatial and Temporal Aggregation of Climatic Input Data. *PLoS ONE* **2016**, *11*. [CrossRef] [PubMed]

73. Wutzler, T.; Reichstein, M. Soils apart from equilibrium—Consequences for soil carbon balance modelling. *Biogeosciences* **2007**, *4*, 125–136. [CrossRef]

74. Müller, U.; Waldeck, A. *Auswertungsmethoden im Bodenschutz-Dokumentation zur Methodenbank des Niedersächsischen Bodeninformationssystems (NIBIS®)*; GeoBerichte Landesamt für Bergbau, Energie, Geologie: Hannover, Germany, 2011; 415p.

75. Wood, S.N. On *p*-values for smooth components of an extended generalized additive model. *Biometrika* **2013**, *100*, 221–228. [CrossRef]

76. Wood, S.N. A simple test for random effects in regression models. *Biometrika* **2013**, *100*, 1005–1010. [CrossRef]

77. *AG-Boden Bodenkundliche Kartieranleitung*; Bundesanstalt für Geowissenschaften und Rohstoffe: Hannover, Germany, 2005; p. 438.

78. Spranger, T.; Lorenz, K.; Gregor, H.-D. *Manual on Methodologies and Criteria for Modelling and Mapping Critical Loads & Levels and Air Pollution Effects, Risks and Trends*; Texte Umweltbundesamt; Federal Environmental Agency (Umweltbundesamt): Berlin, Germany, 2004; 266p.

79. Alveteg, M.; Walse, C.; Warfvinge, P. Reconstructing historic atmospheric deposition and nutrient uptake from present day values using MAKEDEP. *Water Air Soil Pollut.* **1998**, *104*, 269–283. [CrossRef]

80. Builtjes, P.; Hendriks, E.; Koenen, M.; Schaap, M.; Banzhaf, S.; Kerschbaumer, A.; Gauger, T.; Nagel, H.-D.; Scheuschner, T.; Schlutow, A. *Erfassung, Prognose und Bewertung von Stoffeinträgen und ihren Wirkungen in Deutschland (Modelling of Air Pollutants and Ecosystem Impact—MAPESI)*; Texte Umweltbundesamt: Dessau-Rosslau, Germany, 2011; 97p.

81. Tarrasón, L.; Nyíri, Á. *Transboundary Acidification, Eutrophication and Ground Level Ozone in Europe in 2006*; EMEP Status Report; The Norwegian Meteorological Institute: Oslo, Norway, 2008; 136p.

82. Amann, M.; Bertok, I.; Cofala, J.; Heyes, C.; Klimont, Z.; Rafaj, P.; Schöpp, W.; Wagner, F. *National Emission Ceilings for 2020 Based on the 2008 Climate & Energy Package*; NEC Scenario Analysis Report Nr. 6; International Institute for Applied Systems Analysis (IIASA): Laxenburg, Austria, 2008; 72p.

83. R Development Team. *R: A Language and Environment for Statistical Computing*; R Foundation for Statistical Computing: Vienna, Austria, 2015; ISBN 3-900051-07-0. Available online: http://www.R-project.org (accessed on 19 June 2017).

84. Paradis, E.; Claude, J.; Strimmer, K. APE: Analyses of phylogenetics and evolution in R language. *Bioinformatics* **2004**, *20*, 289–290. [CrossRef] [PubMed]

85. Knutti, R. The end of model democracy? *Clim. Chang.* **2010**, *102*, 395–404. [CrossRef]

86. Wechsung, F.; Wechsung, M. Dryer year and brighter sky—The predictable simulation outcomes for Germany's warmer climate from the weather resampling model STARS. *Int. J. Climatol.* **2015**, *35*, 3691–3700. [CrossRef]

87. Wechsung, F.; Wechsung, M. A methodological critique on using temperature-conditioned resampling for climate projections as in the paper of Gerstengarbe et al. (2013) winter storm- and summer thunderstorm-related loss events in Theoretical and Applied Climatology (TAC). *Theor. Appl. Climatol.* **2016**, *126*, 611. [CrossRef]

88. Bloch, R.; Wechsung, F.; Heß, J.; Bachinger, J. Climate change impacts of legume-grass swards: Implications for organic farming in the Federal State of Brandenburg, Germany. *Reg. Environ. Chang.* **2015**, *15*, 405–414. [CrossRef]

89. Keenan, T.F.; Hollinger, D.Y.; Bohrer, G.; Dragoni, D.; Munger, J.W.; Schmid, H.P.; Richardson, A.D. Increase in forest water-use efficiency as atmospheric carbon dioxide concentrations rise. *Nature* **2013**, *499*, 324–327. [CrossRef] [PubMed]

90. Riek, W.; Russ, A. Regionalisierung des Bodenwasserhaushaltes für Klimaszenarien als Grundlage für die forstliche Planung. In Wissenstransfer in die Praxis-Beiträge zum 9. Winterkolloquium. Eberswalder Forstliche Schriftenreihe, Landesbetrieb Forst Brandenburg, Landekompetenzzentrum Forst Eberswalde (Ed.), Eberswalde. 2014, 55, 20–30. Available online: http://forst.brandenburg.de/cms/media.php/lbm1.a.4595.de/efs55.pdf (accessed on 4 May 2016).

91. Agren, G.I.; Bosatta, E. Reconciling differences in predictions of temperature response of soil organic matter. *Soil Biol. Biochem.* **2002**, *34*, 129–132. [CrossRef]

92. Davidson, E.A.; Trumbore, S.E.; Amundson, R. Soil warming and organic carbon content. *Nature* **2000**, *408*, 788–789. [CrossRef] [PubMed]

93. Giardina, G.P.; Ryan, M.G. Evidence that decomposition rates of organic carbon in mineral soil do not vary with temperature. *Nature* **2000**, *404*, 858–861. [CrossRef] [PubMed]

94. Liski, J.; Ilvesniemi, H.; Mäkelä, A.; Westman, C.J. CO_2 emissions from soil in response to climatic warming are overestimated—The decomposition of old soil organic matter is tolerant to temperature. *Ambio* **1999**, *28*, 171–174.

95. Thornley, J.H.M.; Cannell, M.G.R. Soil Carbon Storage Response to Temperature: An Hypothesis. *Ann. Bot.* **2001**, *87*, 591–598. [CrossRef]

96. Farina, R.; Coleman, K.; Whitmore, A.P. Modification of the RothC model for simulations of soil organic C dynamics in dryland regions. *Geoderma* **2013**, *200–201*, 18–30. [CrossRef]

97. Berg, B.; Meentemeyer, V. Litter quality in a north European transect versus carbon storage potential. *Plant Soil* **2002**, *242*, 82–93. [CrossRef]

98. Whitehead, P.G.; Lapworth, D.J.; Skeffington, R.A.; Wade, A. Excess nitrogen leaching and C/N decline in the Tillingbourne catchment, southern England: INCA process modelling for current and historic time series. *Hydrol. Earth Syst. Sci.* **2002**, *6*, 455–466. [CrossRef]

99. De Vries, W.; Reinds, G.J.; Gundersen, P.; Sterba, H. The impact of nitrogen deposition on carbon sequestration in European forests and forest soils. *Glob. Chang. Biol.* **2006**, *12*, 1151–1173. [CrossRef]

100. Mol-Dijkstra, J.; Reinds, G.J.; Kros, H.; Björn, B.; De Vries, W. Modelling soil carbon sequestration of intensively monitored forest plots in Europe by three different approaches. *For. Ecol. Manag.* **2009**, *258*, 1780–1793. [CrossRef]

101. Meiwes, K.J.; Meesenburg, H.; Eichhorn, J.; Jacobsen, C.; Khanna, P.K. Changes in C and N contents of soils under beech forests over a period of 35 years. In *Functioning and Management of European Beech Ecosystems*; Ecol. Studies, 208; Brumme, R., Khanna, P., Eds.; Springer: Berlin, Germany, 2009; pp. 49–63.

102. De Vries, W.; Solberg, S.; Dobbertin, M.; Sterba, H.; Laubhann, D.; van Oijen, M.; Evans, C.; Gundersen, P.; Kros, J.; Wamelink, G.W.W.; et al. The impact of nitrogen deposition on carbon sequestration by European forests and heathlands. *For. Ecol. Manag.* **2009**, *258*, 1814–1823. [CrossRef]

103. Hagedorn, F.; Maurer, S.; Egli, P.; Blaser, P.; Bucher, J.B.; Siegwolf, R. Carbon sequestration in forest soils: Effects of soil type, atmospheric CO_2 enrichment, and N deposition. *Eur. J. Soil Sci.* **2001**, *52*, 619–628. [CrossRef]

104. Kohlpainter, M.; Huber, C.; Weiss, W.; Göttlein, A. Spatial and temporal variability of nitrate concentration in seepage water under a mature Norway sprcue [*Picea abies* (L.) Karst] stand before and after clear cut. *Plant Soil* **2009**, *314*, 285–301. [CrossRef]

105. Kohlpainter, M.; Huber, C.; Göttlein, A. Improving the precision of estimating nitrate (NO3-) concentration in seepage water of forests by prestratification with soil samples. *Eur. J. For. Res.* **2012**. [CrossRef]

106. Manderscheid, B.; Matzner, E. Spatial heterogeneity of soil solution chemistry in a mature Norway spruce (*Picea abies* (L.) Karst.) stand. *Water Air Soil Pollut.* **1995**, *85*, 1185–1190. [CrossRef]

107. Matejek, B.; Kohlpainter, M.; Gasche, R.; Huber, C.; Dannemann, M.; Papen, H. The small-scale pattern of seepage water nitrate concentration in an N saturated spruce forest is regulated by net N mineralization in the organic layer. *Plant Soil* **2008**, *310*, 167–179. [CrossRef]

108. Horváth, B.; Meiwes, K.J.; Meesenburg, H.; Ackermann, J. Nitratausträge unter Wald. Untersuchungen auf Standorten mit hohen luftbürtigen Stickstoffeinträgen. *Grundwasser* **2010**, *9*, 32.

109. Riek, W. Quantifizierung des Risikos für Nitrataustrag aus brandenburgischen Waldökosystemen auf der Grundlage chemischer Oberbodeneigenschaften. In *Wald im Klimawandel-Risiken und Anpassungsstrategien. Eberswalder Forstliche Schriftenreihe*; Landesbetrieb Forst Brandenburg, Landekompetenzzentrum Forst Eberswalde, Ed.; Landesbetrieb Forst Brandenburg: Eberswalde, Germany, 2009; Volume 42, pp. 93–100.

110. Russ, A.; Riek, W.; Martin, J. *Zustand und Wandel der Waldböden Mecklenburg-Vorpommerns-Ergebnisse der zweiten bundesweiten Bodenzustandserhebung in Mecklenburg-Vorpommern*; Mitt. aus dem Forstlichen Versuchswesen Mecklenburg-Vorpommern; Landesforst Mecklenburg-Vorpommern: Schwerin, Germany, 2011; p. 108.

111. Mellert, K.H.; Gensior, A.; Kölling, C. Stickstoffsättigung in den Wäldern Bayerns-Ergebnisse der Nitratinventur. *Forstarchiv* **2005**, *76*, 35–43.

112. Erisman, J.W.; Draaijers, G.P.J. Deposition to forests in Europe: Most important factors influencing dry deposition and models used for generalisation. *Environ. Pollut.* **2003**, *124*, 379–388. [CrossRef]

113. Schaap, M.; Timmermans, R.M.A.; Roemer, M.; Boersen, G.A.C.; Builtjes, P.J.H. The LOTOS–EUROS model: Description, validation and latest developments. *Int. J. Environ. Pollut.* **2008**, *32*, 270–290. [CrossRef]

114. Molina-Herrera, S.; Haas, E.; Grote, R.; Kiese, R.; Klatt, S.; Kraus, D.; Kampffmeyer, T.; Friedrich, R.; Andreae, H.; Loubet, B.; et al. Importance of soil NO emissions for the total atmospheric NOx budget of Saxony, Germany. *Atmos. Environ.* **2017**, *152*, 61–76. [CrossRef]

115. Groffman, P.M.; Tiedje, J.M. Denitrification in north temperate forest soils: Relationships between denitrification and environmental factors at the landscape scale. *Soil Biol. Biochem.* **1989**, *21*, 621–626. [CrossRef]

116. Reinds, G.J.; De Vries, W. Uncertainties in critical loads and target loads of sulphur and nitrogen for European forests: Analysis and quantification. *Sci. Total Environ.* **2010**, *408*, 1960–1970. [CrossRef] [PubMed]

117. Schneider, S. CO$_2$, Climate and Society: A Brief Overview. In *Social Science Research and Climate Change*; Chen, R., Boulding, E., Schneider, S., Eds.; Springer: Dordrecht, The Netherlands, 1983; pp. 9–15.

118. Reyer, C. The Cascade of Uncertainty in Modeling Forest Ecosystem Responses to Environmental Change and the Challenge of Sustainable Resource Management. Ph.D. Thesis, Humboldt-Universität, Berlin, Germany, 2013.

119. Stuart, M.E.; Gooddy, D.C.; Bloomfield, J.P.; Williams, A.T. A review of the impact of climate change on future nitrate concentrations in groundwater of the UK. *Sci. Total Environ.* **2011**, *409*, 2859–2873. [CrossRef] [PubMed]

120. Dirnböck, T.; Kobler, J.; Kraus, D.; Grote, R.; Kiese, R. Impacts of management and climate change on nitrate leaching in a forested karst area. *J. Environ. Manag.* **2016**, *165*, 243–252. [CrossRef] [PubMed]

121. Sverdrup, H.; Warfvinge, P. Calculating field weathering rates using a mechanistic geochemical model PROFILE. *Appl. Geochem.* **1993**, *8*, 273–283. [CrossRef]

122. Ahrends, B. Dynamische Modellierung der Auswirkungen von Kalkungen und Nutzungsszenarien auf die Basensättigung im Wurzelraum. *Beiträge aus der Nordwestdeutschen Forstlichen Versuchsanstalt* **2012**, *9*, 95–114.

123. Bonten, J. MetHyd: A Meteo-Hydrological Pre-Processor for VSD+. Version 1.5.1. 2013. Available online: http://wge-cce.org/Methods_Models/Available_Models (accessed on 21 November 2013).